

1
2 **A Phenomenology of New Particle Formation (NPF) at**
3 **Thirteen European Sites**
4

5 **Dimitrios Bousiotis¹, Francis D. Pope¹, David C. Beddows¹,**
6 **Manuel Dall'Osto², Andreas Massling³, Jacob Klenø Nøjgaard^{3,4},**
7 **Claus Nordstrøm³, Jarkko V. Niemi⁵, Harri Portin⁵, Tuukka Petäjä⁶,**
8 **Noemi Perez⁷, Andrés Alastuey⁷, Xavier Querol⁷, Giorgos Kouvarakis⁸,**
9 **Stergios Vratolis⁹, Konstantinos Eleftheriadis⁹, Alfred Wiedensohler¹⁰,**
10 **Kay Weinhold¹⁰, Maik Merkel¹⁰, Thomas Tuch¹⁰ and Roy M. Harrison^{1*†}**
11

12 **¹Division of Environmental Health and Risk Management**
13 **School of Geography, Earth and Environmental Sciences**
14 **University of Birmingham, Edgbaston, Birmingham B15 2TT, United Kingdom**
15

16 **²Institute of Marine Sciences**
17 **Passeig Marítim de la Barceloneta, 37-49, E-08003, Barcelona, Spain**
18

19 **³Department of Environmental Science, Aarhus University, 4000 Roskilde, Denmark**
20

21 **⁴The National Research Centre for the Working Environment, 2100 Copenhagen, Denmark**
22

23 **⁵Helsinki Region Environmental Services Authority (HSY),**
24 **FI-00066 HSY, Helsinki, Finland**
25

26 **⁶Institute for Atmospheric and Earth System Research (INAR) / Physics, Faculty of Science,**
27 **University of Helsinki, Finland**
28

29 **⁷Institute of Environmental Assessment and Water Research (IDAEA - CSIC), 08034,**
30 **Barcelona, Spain**
31

32 **⁸Environmental Chemical Processes Laboratory (ECPL), Department of Chemistry,**
33 **University of Crete, 70013, Heraklion, Greece**

* To whom correspondence should be addressed (Email: r.m.harrison@bham.ac.uk)

†Also at: Department of Environmental Sciences / Center of Excellence in Environmental Studies, King Abdulaziz University, PO Box 80203, Jeddah, 21589, Saudi Arabia

34
35
36
37
38
39
40
41
42

⁹Environmental Radioactivity Laboratory, Institute of Nuclear and Radiological Science & Technology, Energy & Safety, NCSR Demokritos, Athens, Greece

**¹⁰Leibniz Institute for Tropospheric Research (TROPOS),
Permoserstr. 15, 04318 Leipzig, Germany**

43 **ABSTRACT**

44 New particle formation (NPF) events occur almost everywhere in the world and can play an
45 important role as a particle source. The frequency and characteristics of NPF events vary spatially
46 and this variability is yet to be fully understood. In the present study, long term particle size
47 distribution datasets (minimum of three years) from thirteen sites of various land uses and climates
48 from across Europe were studied and NPF events, deriving from secondary formation and not
49 traffic related nucleation, were extracted and analysed. The frequency of NPF events was
50 consistently found to be higher at rural background sites, while the growth and formation rates of
51 newly formed particles were higher at roadsides (though in many cases differences between the
52 sites were small), underlining the importance of the abundance of condensable compounds of
53 anthropogenic origin found there. The growth rate was higher in summer at all rural background
54 sites studied. The urban background sites presented the highest uncertainty due to greater variability
55 compared to the other two types of site. The origin of incoming air masses and the specific
56 conditions associated with them greatly affect the characteristics of NPF events. In general, cleaner
57 air masses present higher probability for NPF events, while the more polluted ones show higher
58 growth rates. However, different patterns of NPF events were found even at sites in close proximity
59 (< 200 km) due to the different local conditions at each site. Region-wide events were also studied
60 and were found to be associated with the same conditions as local events, although some variability
61 was found which was associated with the different seasonality of the events at two neighbouring
62 sites. NPF events were responsible for an increase in the number concentration of ultrafine particles

63 of more than 400% at rural background sites on the day of their occurrence. The degree of
64 enhancement was less at urban sites due to the increased contribution of other sources within the
65 urban environment. It is evident that, while some variables (such as solar radiation intensity,
66 relative humidity or the concentrations of specific pollutants) appear to have a similar influence on
67 NPF events across all sites, it is impossible to predict the characteristics of NPF events at a site
68 using just these variables, due to the crucial role of local conditions.

69

70 **Keywords:** Nucleation; New Particle Formation; Ultrafine Particles; Roadside; Urban Background;

71 Rural

72

73 1. INTRODUCTION

74 Ultrafine particles (particles with diameter smaller than 100 nm), while not yet regulated, are
75 believed to have adverse effects upon air quality and public health (Atkinson et al., 2010; Politis et
76 al., 2008; Tobías et al., 2018), as well as having a direct or indirect effect on atmospheric properties
77 (Makkonen et al., 2012; Seinfeld and Pandis, 2012). The source of ultrafine particles can either be
78 from primary emissions (Harrison et al., 2000; Masiol et al., 2017), including delayed primary
79 emissions (Hietikko et al., 2018; Olin et al., 2020; Rönkkö et al., 2017), or from secondary
80 formation from gaseous precursors (Brean et al., 2019; Chu et al., 2019; Kerminen et al., 2018;
81 Kulmala et al., 2004a; Yao et al., 2018), which is considered as an important source of CCN in the
82 atmosphere (Dameto de España et al., 2017; Kalivitis et al., 2015; Spracklen et al., 2008). For the
83 latter, while the process of formation of initial clusters that subsequently lead to particle formation
84 has been extensively studied (Dal Maso et al., 2002; Kulmala et al., 2014; Riipinen et al., 2007;
85 Weber et al., 1998), there is no consistent explanation of the factors which determine the occurrence
86 and development of NPF events in the atmosphere. Additionally, events that resemble NPF, with
87 the initial particles deriving from primary emissions, especially close to traffic sources (Rönkkö et
88 al., 2017), have been also reported but these are out of the scope of the present study.

89

90 A large number of studies both in laboratories and in real world conditions have been conducted to
91 either describe or explain the mechanisms that drive NPF events. The role of meteorological
92 conditions, such as solar radiation intensity (Kumar et al., 2014; Shi et al., 2001; Stanier et al.,

93 2004) and relative humidity (Li et al., 2019; Park et al., 2015), are well documented, while great
94 diversity was found for the effect of other meteorological factors such as the wind speed (Charron et
95 al., 2008; Németh and Salma, 2014; Rimnácová et al., 2011) or temperature (Jeong et al., 2010;
96 Napari et al., 2002). There are also influences of atmospheric composition, with the positive role of
97 low condensation sink and concentrations of pollutants such as NO_x upon NPF event occurrence
98 being widely agreed upon (Alam et al., 2003; Cheung et al., 2013; Kerminen et al., 2004; Wang et
99 al., 2014; Wehner et al., 2007). Contrary to that, while the indirect role of SO₂ is well established in
100 the nucleation process, via the formation of new clusters of H₂SO₄ molecules (Boy et al., 2005; Iida
101 et al., 2008; Kulmala et al., 2005; Sipila et al., 2010; Xiao et al., 2015), uncertainty exists in the role
102 that different concentrations of SO₂ play in the occurrence of NPF events in real world atmospheric
103 conditions (Alam et al., 2003; Dall'Osto et al., 2018; Wonaschütz et al., 2015; Woo et al., 2001).
104 Ammonia is known to enhance the formation of initial clusters (Korhonen et al., 1999; Ortega et al.,
105 2008; Schobesberger et al., 2015), and volatile organic compounds are regarded as the main drivers
106 of the growth of the newly formed particles (Kulmala et al., 2013; Riccobono et al., 2014; Tröstl et
107 al., 2016). NPF events in different locations do not appear to follow consistent trends with the
108 concentrations of these compounds and meteorological parameters (McFiggans et al., 2019;
109 Minguillón et al., 2015; Riipinen et al., 2007), though links between NPF events and sulphuric acid
110 vapour concentrations (Petäjä et al., 2009; Weber et al., 1995) and organics (Bianchi et al., 2019;
111 Ehn et al., 2014) have been reported.

112

113 It is evident that NPF events and their development are complex, and local conditions play an
114 important role in their variability. Many studies have attempted to explain this variability by
115 analyzing multiple datasets from wider areas. Studies in the UK (Bousiotis et al., 2019; Hama et al.,
116 2017), Spain (Brines et al., 2014; Carnerero et al., 2018; Dall'Osto et al., 2013; Minguillón et al.,
117 2015), Hungary (Németh and Salma, 2014; Salma et al., 2014, 2016), Greece (Kalkavouras et al.,
118 2017; Siakavaras et al., 2016), Germany (Costabile et al., 2009; Ma and Birmili, 2015; Sun et al.,
119 2019) and China (Peng et al., 2017; Shen et al., 2018; Wang et al., 2017) have attempted to explain
120 the differences found in NPF event conditions and variability between different sites in close
121 proximity, while larger scale studies using descriptive (Brines et al., 2015; Hofman et al., 2016;
122 Jaatinen et al., 2009; Kulmala et al., 2005) or statistical methods (Dall'Osto et al., 2018; Rivas et
123 al., 2020) have provided insights into the effect of the variability of parameters that are considered
124 to play an important role in the occurrence and development of NPF events on a broader scale.

125

126 The present study, combining thirteen long term datasets (minimum of three years) from different
127 countries across Europe and combined with the results from a previous study in the UK, attempts to
128 elucidate the effect of the local conditions on NPF event characteristics (frequency of NPF events,
129 formation rate and growth rate) both for sites in close proximity (< 200 km), and by
130 intercomparison of sites on a continental scale in order to find general trends of the variables that
131 affect the characteristics and development of NPF events on a larger scale. Finally, the effect of

132 NPF events upon the ultrafine particle number concentrations was calculated, providing insight to
133 the potential of NPF events to influence the local air quality conditions in all areas studied.

134

135 **2. DATA AND METHODS**

136 **2.1 Site Description and Data Availability**

137 In the present study, particle number size distribution data from 13 sites in Europe (Figure 1) are
138 analysed in the size range $3 \text{ nm} < D_p < 1000 \text{ nm}$. A detailed list of the site locations and the data
139 available for each is found in Table 1 (seasonal data availability is found in Table S1). For site naming
140 the first three letters refer to the country (DEN = Denmark, GER = Germany, FIN = Finland, SPA =
141 Spain, GRE = Greece) while the next two refer to the type of site (RU = Rural background, UB =
142 Urban background, RO = Roadside). Average meteorological conditions and concentrations of
143 chemical compounds for all sites are found in Tables S2 and S3 respectively; their seasonal variation
144 is found in Table S4.

145

146 **2.2 Methods**

147 **2.2.1 NPF event selection**

148 The identification of NPF events was conducted manually using the criteria set by Dal Maso et al.
149 (2005). According to these, a NPF event is considered to occur when:

- 150 • a distinctly new mode of particles appears in the nucleation range,
- 151 • this new mode prevails for some hours,

152 • the new mode shows signs of growth.

153

154 The NPF events extracted using this method are then classified into classes I or II depending on the
155 level of confidence. Class I (high confidence) is further classified as Ia and Ib, with class Ia
156 containing the events that both present a clear formation of a new mode as well as a distinct growth
157 of this mode, while Ib includes those with a less distinct formation and development. In the present
158 study, only the events classified as Ia were used as they are considered as more suitable for study.
159 As the growth criterion is not fully defined, in the present study a minimum growth rate of 1 nm h^{-1}
160 is required for NPF events to be considered. The events found using this method should not be
161 confused with the formation and growth of particles deriving from primary emissions next to
162 pollution sources, such as traffic. While to an extent the particle formation found can be biased by
163 primary emissions (especially at roadside sites), great effort was made using additional data, such as
164 atmospheric composition data, to not include any incidents of traffic related nucleation.

165

166 **2.2.2 Calculation of condensation sink, growth rate, formation rate, Nucleation Strength** 167 **Factor (NSF) and NPF event probability**

168 The calculation of the condensation sink was made using the method proposed by Kulmala et al.
169 (2001). The condensation sink (CS) is calculated as:

170

$$171 \text{ CS} = 4\pi D_{vap} \sum \beta_M r N$$

172 where r and N are the radius and the number concentration of the particles and D_{vap} is the diffusion
173 coefficient, calculated for $T = 293$ K and $P = 1013.25$ mbar, according to Poling et al. (2001):

174

$$175 \quad D_{\text{vap}} = 0.00143 \cdot T^{1.75} \frac{\sqrt{M_{\text{air}}^{-1} + M_{\text{vap}}^{-1}}}{P \left(D_{x,\text{air}}^{\frac{1}{3}} + D_{x,\text{vap}}^{\frac{1}{3}} \right)^2}$$

176

177 where M and D_x are the molar mass and diffusion volume for air and H_2SO_4 . β_M is the Fuchs
178 correction factor calculated from Fuchs and Sutugin (1971):

179

$$180 \quad \beta_M = \frac{1 + K_n}{1 + \left(\frac{4}{3a} + 0.377 \right) K_n + \frac{4}{3a} K_n^2}$$

181

182 K_n is the Knudsen number, defined as $K_n = 2\lambda_m/d_p$, with λ_m being the mean free path of the gas.

183

184 The growth rate of the newly formed particles is calculated according to Kulmala et al. (2012), as

185

$$186 \quad \text{GR} = \frac{D_{P_2} - D_{P_1}}{t_2 - t_1}$$

187

188 for the size range between the minimum available particle diameter up to 30 nm. For the calculation
 189 of the growth rate, the time considered was from the start of the event until a) growth stopped, b)
 190 GMD reached the upper limit set or c) the day ended. Due to the differences in the smallest particle
 191 size available between the sites, a discrepancy would exist for the growth rate values presented
 192 (sites with lower size cut would present lower values of growth rate, as the growth rate tends to
 193 increase with particle size in this range (Deng et al., 2020)). As a result, a direct comparison of the
 194 growth rate values found among sites with significant differences at the smallest particle size
 195 available was avoided.

196

197 The formation rate J was calculated using the method proposed by Kulmala et al. (2012) in which:

198

$$199 \quad J_{d_p} = \frac{dN_{d_p}}{dt} + \text{CoagS}_{d_p} \times N_{d_p} + \frac{GR}{\Delta d_p} \times N_{d_p} + S_{\text{losses}}$$

200

201 where CoagS_{d_p} is the coagulation rate of particles of diameter d_p , calculated by:

202

$$203 \quad \text{CoagS}_{d_p} = \int K(d_p, d'_p) n(d'_p) dd'_p \cong \sum_{d'_p=d_p}^{d'_p=\text{max}} K(d_p, d'_p) N_{d_p}$$

204

205 as proposed by Kerminen et al. (2001). $K(d_p, d'_p)$ is the coagulation coefficient of particle sizes d_p
206 and d'_p . S_{losses} accounts for the additional loss terms (i.e. chamber walls), not considered here. Initial
207 particle formation starts at about 1.5 ± 0.4 nm (Kulmala et al., 2012). The formation rate calculated
208 here refers to particles in the atmosphere that reached the diameter of 10 nm during NPF events for
209 uniformity reasons. This means that these particles were formed earlier during the day of the events,
210 survived and grew to this size later in the day. Furthermore, due to the effect of the morning rush
211 which biased the results at roadsides, the averages are calculated for the time window between 9:00
212 to 15:00 (± 3 hours from noon, when J_{10} peaked in the majority of the events). This was done for all
213 the sites in this study for consistency.

214
215 As mentioned in the methodology for NPF event selection (chapter 2.2.1) days with particle
216 formation resulting directly from traffic emissions were excluded. For those identified as NPF event
217 days though, mainly for the roadside sites, ~~such~~ formation associated with traffic emissions still
218 occurs. It is impossible with the data available for this study to remove the traffic related particle
219 formation in the calculations included in this study, by effectively separating it from secondary
220 particle formation or calculate it. Using average conditions for comparison would lead to negative
221 formation rate values in most cases, since in order for an NPF event to occur, ~~other emission~~traffic
222 related particles are usually reduced to a greater extent compared to the formation from NPF,
223 leading to lower particle concentrations on event days as found from a previous study in
224 Marylebone Road, London (Bousiotis et al., 2019). This may result in an overestimation of the

225 formation rates at roadside sites presented in this study, ~~which, as mentioned earlier, was reduced as~~
226 ~~far as possible by choosing~~ The choice of a time window for which we would have the maximum
227 effect of secondary particle formation and the minimum possible effect from traffic related particle
228 formation attempts to reduce this discrepancy as much as possible.

229
230 The Nucleation Strength Factor (NSF) proposed by Nemeth and Salma (2014) is a measure of the
231 effect of NPF events on ultrafine particle concentration. It can either refer to the effect of NPF
232 events on the day of their occurrence, calculated by:

$$234 \text{ NSF}_{\text{NUC}} = \frac{\left(\frac{N_{\text{smallest size available}-100\text{nm}}}{N_{100\text{nm}-\text{largest size available}}} \right)_{\text{nucleation days}}}{\left(\frac{N_{\text{smallest size available}-100\text{nm}}}{N_{100\text{nm}-\text{largest size available}}} \right)_{\text{non-nucleation days}}}$$

235
236 or their overall contribution on the ultrafine particle concentrations at a site calculated by:

$$238 \text{ NSF}_{\text{GEN}} = \frac{\left(\frac{N_{\text{smallest size available}-100\text{nm}}}{N_{100\text{nm}-\text{largest size available}}} \right)_{\text{all days}}}{\left(\frac{N_{\text{smallest size available}-100\text{nm}}}{N_{100\text{nm}-\text{largest size available}}} \right)_{\text{non-nucleation days}}}$$

239
240 The NPF event probability is a simple metric of the probability of NPF events calculated by the
241 number of NPF event days divided by the number of days with available data for the given group

242 (temporal, wind direction etc.). Finally, it should be mentioned that all the results presented are
243 normalised according the seasonal data availability for each site, based upon the expression:

$$244 \text{ NPF}_{probability} = \frac{N_{NPF \text{ event days for group of days } X}}{N_{days \text{ with available data for group of days } X}}$$

245

246 **3. RESULTS**

247 The seasonal NPF probability for all sites is found in Table S5. The annual number of NPF events,
248 growth rate and formation rate for all the sites is found in Table S6, for which no clear interannual
249 trend is found for any of the sites in this study. This may be due to the relatively short period of
250 time studied for such variations to be observed.

251

252 **3.1 Frequency and Seasonality of NPF Events**

253 In Denmark, NPF events occurred at all three sites with a similar frequency for the urban sites
254 (5.4% for DENRO and 5.8% for DENUB) and higher for the rural DENRU site (7.9%). The
255 seasonal variation favoured summer at DENRU and DENRO, while at DENUB a similar frequency
256 for spring and summer was found (Figure 2). The within-week variation of the events favours
257 weekends compared to weekdays going from the rural background site to the roadside site (Figure
258 3). Interesting is the increased frequency of NPF events found in all Danish sites on Thursday
259 among the weekdays. This trend though does not have a plausible explanation and is probably
260 coincidental.

261

262 A higher frequency of events for all types of environments is found for the German sites compared
263 to all other countries in this study. The background sites had NPF events for more than 17% of the
264 days, while the roadside had a lower frequency of about 9%, with a seasonal variability favouring
265 summer at all sites. It should be noted though that, due to the lack of spring and summer data for the
266 first two years at the German roadside site, the frequency of events is probably a lot higher, and the
267 seasonal variation should further favour these seasons. No substantial within-week variation was
268 found for any of the sites in this country, a feature that is expected mainly at background sites. For
269 GERRO, this may be due to not being as polluted as other sites of the same type, having an average
270 condensation sink comparable to that of urban background sites in this study.

271

272 NPF events at the sites in Finland presented the most diverse seasonal variation, peaking at the
273 background sites in spring and at the roadside site in summer (while the spring data availability is
274 somewhat reduced for the Finnish roadside site, the general trend remains the same if all seasons
275 had the same data availability). The frequency of NPF events at FINRU was higher (8.66%)
276 compared to the urban sites (4.97% at FINUB and 5.20% at FINRO). Strong within-week variation
277 favouring weekends is found for the roadside site, while no clear variation was found for the
278 background sites. This may be due to either the higher condensation sink during weekdays that
279 suppresses the events, or the dominant impact of the traffic emissions which could make the
280 detection of NPF events harder.

281

282 For Spain, data was available for an urban and a rural background site in the greater area of
283 Barcelona. NPF events were rather frequent, occurring on about 12% of the days at the rural
284 background site and 13.1% at the urban site. Though the sites are in close proximity (about 50 km),
285 the seasonality of NPF events was different between them, peaking in spring at SPARU and autumn
286 at SPAUB. The frequency of NPF events in winter was relatively high compared to the sites in
287 central and northern Europe and higher than summer for both sites. For both sites a higher NPF
288 probability was found on weekends compared to weekdays, though this trend is stronger at SPAUB.
289 Finally, for Greece data are available for two background sites, though not in close proximity (the
290 distance between the sites is about 350 km). While in Greece meteorological conditions are
291 favourable in general for NPF events, with high solar radiation and low relative humidity, their
292 frequency was only 8.5% for the urban background site in Athens and 6.5% for the rural
293 background site in Finokalia, similar to the frequency of Class I events reported in the study by
294 Kalivitis et al. (2019). Most NPF events occurred in spring at both sites, peaking in April. It is
295 interesting that the sites in southern Europe (in Spain and Greece) have a considerable number of
296 NPF events during winter, which might be due to the specific meteorological conditions found in
297 this area, where winter is a lot warmer than at the sites in northern and central Europe, and
298 insolation is higher.

299
300
301

302 3.2 The Formation and Growth Rates

303 For the Danish sites the growth rate was found to be higher at the roadside site at $4.45 \pm 1.87 \text{ nm h}^{-1}$
304 and it was similar for the other two sites (3.19 ± 1.43 for DENRU and 3.19 ± 1.45 for DENUB) nm h^{-1}
305 (Figure 4), though the peak was found in different seasons (Figure 5), coinciding with that of the
306 frequency of NPF events (the highest average for DENRO was found for winter but it was only for
307 a single event that occurred in that season). The formation rate (J_{10}) was found to be broadly similar
308 at the rural and urban background sites and higher at DENRO (Figure 6), favoured by different
309 seasons at each site (summer at DENRU, spring at DENUB though with minimal differences and
310 autumn at DENRO) (Figure 7).

311

312 Similar to the frequency of NPF events, the German sites also had higher growth rates compared to
313 sites of the same type in other areas of this study, with GERRU having $4.34 \pm 1.73 \text{ nm h}^{-1}$, GERUB
314 $4.24 \pm 1.69 \text{ nm h}^{-1}$ and GERRO $5.17 \pm 2.20 \text{ nm h}^{-1}$ (Figure 3). While the difference between GERRU
315 and GERUB is not statistically significant, there is a significant difference with GERRO ($p <$
316 0.005). Higher growth rates were found in summer compared to spring for all sites (Figure 5).
317 Specifically, for the roadside though, the highest average growth rates were found in autumn, which
318 may be either a site-specific feature or an artefact of the limited number of events in that season
319 (total of 11 NPF events in autumn). Similarly, J_{10} at the German sites was also the highest among
320 the sites of this study, increasing from the GERRU to GERRO. It was found to be higher in summer
321 for the background sites and in autumn for GERRO.

322 For the Finnish sites, growth rates were similar at the background sites ($2.91 \pm 1.68 \text{ nm h}^{-1}$ at FINRU
323 and $2.87 \pm 1.33 \text{ nm h}^{-1}$ at FINUB), peaking in the summer months, similar to the findings of Yli-Juuti
324 et al. (2011), while the peak for FINRO (growth rate at $3.74 \pm 1.48 \text{ nm h}^{-1}$) was found in spring,
325 though the differences between the seasons for this site were rather small. The formation rate was
326 the highest at FINRO, peaking in autumn for both urban sites (with small differences with spring),
327 while FINRU presented the highest J_{10} in summer.

328

329 At the Spanish sites, the growth rate was similar for the two sites, being $3.62 \pm 1.86 \text{ nm h}^{-1}$ at
330 SPARU and $3.38 \pm 1.53 \text{ nm h}^{-1}$ at SPAUB, again being higher in autumn for the urban site (which
331 appears to be a feature of more polluted sites), while the rural site follows the general trend of rural
332 background sites, peaking in summer. The formation rate at SPAUB is comparable to the other
333 urban background sites (apart from GERUB) and peaked in spring, while once again the peak at
334 SPARU was found in summer, similar to the other rural sites of this study apart from the Greek. At
335 the urban site both the growth and formation rates were higher on weekdays compared to weekends
336 (both $p < 0.001$). While the higher growth rate during weekdays may be associated with the
337 increased presence of condensable species from anthropogenic activities, the higher formation rate
338 might be affected by the increased emissions during these days, which bias to an extent its value.
339 Finally, the growth rate of particles was found to be similar at both Greek sites ($3.68 \pm 1.41 \text{ nm h}^{-1}$
340 for GREUB and $3.78 \pm 2.01 \text{ nm h}^{-1}$ for GRERU) and was higher in summer compared to the other
341 seasons, having a similar trend with the temperature and particulate organic carbon concentrations

342 in the area. The formation rate presented a unique trend, having high averages in winter for both
343 sites. Interestingly, contrary to most background sites in this study, the lowest average J_{10} was found
344 for summer at both sites.

345

346 **3.3 Conditions Affecting NPF Events**

347 The average and NPF event day conditions are presented in tables S2 and S3 (for meteorological
348 conditions and atmospheric composition respectively). A number of variables present consistent
349 behaviour on NPF days. For all the sites in this study the solar radiation intensity was higher on
350 NPF days compared to the average conditions, while the relative humidity was lower. Additionally,
351 all the chemical compounds with available data present either lower or similar concentrations. This
352 is consistent even for the chemical compounds which are associated with the NPF process (such as
353 the SO_2). This probably indicates that they are in sufficient concentrations for not being a limiting
354 factor in the occurrence of the events, while higher concentrations are associated with increased
355 pollution conditions which may suppress their occurrence. The exceptions found are SPARU and
356 GRERU for NO_2 and FINRU for SO_2 . In these sites the concentrations of these gaseous components
357 are very low in general (being rural background sites) and were found to be only marginally higher
358 on NPF event days. These differences indicate that the variability of these compounds is not playing
359 a significant role in the occurrence of the events and thus should not be considered as an important
360 factor. The ozone concentration though, was found to be consistently higher on event days
361 compared to the average conditions at all sites regardless of their geographical location and type. As

362 the ozone concentration variability is directly associated with the solar radiation intensity, it is
363 unknown whether it plays a direct role in the occurrence of the events or it is the result of its
364 covariance with the solar radiation intensity.

365

366 Following that, differences were found in the variability of some of the meteorological conditions,
367 as well as local conditions (either meteorological or specific pollution sources), which played a
368 significant role in the occurrence and the metrics of NPF events across the sites of this study. These
369 will be further explored in the following sections.

370

371 **3.3.1 Denmark**

372 The meteorological conditions that prevailed on NPF event days followed the general trend
373 mentioned earlier, while wind speed and temperature were higher than average (consistently at all
374 sites, meteorological condition variability was significant for all ($p < 0.001$) except the wind speed).
375 As meteorological data were available from the urban background site (the variation between the
376 rural and urban sites should not be great since they are about 25 km away from each other), the
377 average conditions for the three sites are almost the same, with the only variability being the data
378 availability among the sites. Thus, the more common wind directions in the area are southwesterly;
379 for all sites though the majority of NPF events are associated with direct westerly and northwesterly
380 winds, similar to the findings of Wang et al. (2013) for the same site, which are those with the
381 lowest concentrations of pollutants and condensation sink for all sites (Table S7), probably being of

382 marine origin as elemental concentrations showed an increased presence of Na, Cl and Mg (results
383 not included). The wind directions with the highest probability for NPF events presented low
384 growth rates and vice versa (Table S4), though it was proposed by Kristensson et al. (2008) that
385 there is a possibility for events observed at the nearby Vavihill site in Sweden with northwesterly
386 winds to be associated to the emissions of specific ship lanes that pass from that area. Wind
387 direction sectors with higher concentrations of OC coincide with higher growth rates at DENRO,
388 while this variability is not found at DENRU possibly showing that different compounds and
389 mechanisms take part in the growth process of the newly formed particles (Kulmala et al., 2004b).
390

391 As mentioned earlier, DENUB although close to the DENRO site has different seasonal variation of
392 NPF events, with a marginally lower frequency in summer compared to the other two Danish sites,
393 which have almost the same seasonal variation of NPF events. At DENUB, a strong presence of
394 particles in the size range of about 50 – 60 nm is observed (Figure S1), especially during summer
395 months, increasing the condensation sink in the area (this enhanced mode of particles is visible at
396 DENRO as well, but its effect is dampened due to the elevated particle number concentrations in
397 the other modes). This mode is probably part of the urban particle background. The strongest source
398 though at DENUB appears to be from the east and consistently appears at both urban sites; this
399 sector is where both elevated pollutant concentrations and condensation sink are found. In this
400 sector, there are two possible local sources, either the port located 2 km to the east or the power
401 plant located at a similar distance (or both). In general, both stations are located only a few

402 kilometres away from the Øresund strait, a major shipping route. Studying the SMPS plots it can be
403 seen that NPF events at DENUB, especially in summer, tend to start but are either suppressed after
404 the start or have a lifetime of a couple of hours before the new particles are scavenged or evaporate.
405 While this might explain to an extent the frequency and variability of NPF events at this site, the
406 balance between the condensation sink and the concentration of condensable compounds is
407 highlighted. While at DENRO the condensation sink is considerably higher than at DENUB and the
408 effect of the aforementioned mode of particles is present at both, the occurrence and development of
409 NPF events at DENRO are more pronounced in the data, due to the higher concentrations of
410 condensable compounds.

411

412 **3.3.2 Germany**

413 Compared to the average conditions, a higher temperature was found on NPF event days, while
414 wind speed was lower at all German sites. The condensation sink was also higher on event days
415 compared to the average, though this may be the result of the high formation rates found for the
416 German sites. The wind profile is different between the urban and the rural sites, with mainly
417 northeasterly and southwesterly winds at the rural site and a more balanced profile for the urban
418 sites. This difference is probably due to differences in the local topography. For the urban sites the
419 majority of NPF events are associated with easterly winds (to a lesser extent westerly as well for
420 GERRO). At GERUB, along with the increased frequency of NPF events, the highest average
421 growth rate is also found with easterly wind directions (though the differences are rather small). At

422 GERRO the frequency and growth rate appear to be affected by the topography of the site.
423 Eisenbahnstraße is a road with an axis at almost $90^\circ - 270^\circ$ and although the H/W ratio
424 (surrounding building height to width ratio) is not high, the effect of a street canyon vortex is
425 observed (Voigtländer et al., 2006). Possibly as a consequence of this, the probability of NPF events
426 is low for direct northerly and southerly winds, although there are high growth rates of the newly
427 formed particles (highest growth rates observed with southerly winds, associated with cleaner air).
428

429 At GERRU an increased probability of NPF events and growth rate are also found for wind
430 directions from the easterly sector, although these are not very frequent for this site. For this site
431 chemical composition data for $PM_{2.5}$ and PM_{10} are available, and it is found that the generally low
432 (on average) concentrations of pollutants (such as elemental carbon, nitrate and sulphate), in general
433 are elevated for wind directions from that sector. This is also reported for the Melpitz site (GERRU)
434 by Jaatinen et al. (2009) and probably indicates that in a relatively clean area, the presence of low
435 concentrations of pollutants may be favourable in the occurrence and development of NPF events,
436 as in general pollutant concentrations are lower on NPF event days compared to average conditions.
437 Another interesting point is the concentration of organic carbon at the site (average of $2.18 \mu\text{g m}^{-3}$
438 in $PM_{2.5}$), having the highest average concentration among the rural background sites studied. As
439 other pollutant concentrations are relatively low at this site, it is possible that a portion of this
440 organic carbon is of biogenic origin, considering also that the area is largely surrounded by forests
441 and green areas, with a minimal effect of marine air masses (as indicated by the low marine

442 component concentrations – data not included) and possibly pointing to increased presence of
443 BVOCs. The increased presence of organic species at GERRU may explain to some extent the
444 increased frequency of NPF events as well as the highest growth and formation rates found among
445 the sites of this study.

446

447 **3.3.3 Finland**

448 At the background sites in Finland, temperature was lower on NPF event days compared to the
449 average conditions, whereas it was higher for FINRO associated with the different seasonality of
450 the events. No significant differences were found for the wind speed on NPF events for all sites.
451 There are though some significant differences in the wind conditions for NPF events compared to
452 average conditions. At FINRU, NPF events were more common with northerly wind directions, as
453 was also found by Nieminen et al. (2014) and Nilsson et al. (2001). This is probably due to the
454 lower condensation sink which can be associated with the lower relative humidity also found for
455 incoming winds from that sector and explains the lower temperatures found with NPF events at this
456 site. Similarly, at FINUB NPF events were favoured by wind directions from the northerly sector,
457 while there is almost a complete lack of NPF on southerly winds. This is due to its position at the
458 north of both the city centre and the harbour, though winds from that sector are not common in
459 general for that site. Finally, the wind profile for NPF events at FINRO also favours northerly winds
460 with an almost complete absence of NPF in southerly winds, probably due to the elevated pollutant
461 concentrations and condensation sink associated with them.

462 At all sites, NPF event days had a lower condensation sink compared to the average for the site. The
463 seasonal variation of NPF events in Finland favouring spring, was explained by earlier work as the
464 result of the seasonal variation of H₂SO₄ concentrations (Nieminen et al., 2014), which in the area
465 peak in spring. The variation of H₂SO₄ concentrations is directly associated with SO₂ concentrations
466 in the area, which follow a similar trend. The seasonal variation of NPF events at FINRO though
467 cannot be explained by the variation of H₂SO₄ in the area. SO₂ concentrations, which were available
468 only for the nearby urban background site at Kalio (about 3 km away from FINRO) and may
469 provide information upon the trends of SO₂ in the greater area, peak during January (probably due
470 to increased heating in winter and the limited oxidation processes due to lower incoming solar
471 radiation) and are higher during spring months compared to summer. In general, the variation of
472 pollutant concentrations and the condensation sink is not great for the spring and summer seasons.
473 The only variable out of the ones considered that may explain to an extent the seasonality of NPF
474 events at the site is the increased concentrations of PM₁₀ found for spring months, which might be
475 associated with road sanding and salting that takes place in Scandinavian countries during the
476 colder months (Kupiainen et al., 2016) with emissions to the ambient air during spring months
477 (Stojiljkovic et al., 2019). The source of these particles though is uncertain, as no major differences
478 in the wind roses are found between the two seasons. Another study by Sarnela et al. (2015) at a
479 different site in southern Finland attributed the seasonality of NPF events in Finland to the absence
480 of H₂SO₄ clusters during summer months due to a possible lack of stabilizing agents (e.g.
481 ammonia). This could explain the limited number of small particles (smaller than 10 nm) at the

482 background sites during summer. In the more polluted environment at a roadside site these agents
483 may exist, but such data was unfortunately not available.
484

485 Finally, a feature mentioned by Hao et al. (2018) in their study at the site of Hyytiälä, in which late
486 particle growth is observed was also found in this study. This happened on about 20% of NPF days
487 at FINRU (and a number of non-event days) and in most cases in early spring (before mid-April) or
488 late autumn (after mid-September). New particles were formed and either did not grow or grew very
489 slowly until later in the day when growth rates increased (Figure S2). In all these cases, growth
490 started when solar radiation was very low or zero, which probably associates the growth of particles
491 with nighttime chemistry leading to the formation of organonitrates (as found by the same study). A
492 similar behaviour was also occasionally found at FINUB. Particle growth at late hours is not a
493 unique feature for the Finnish sites, as it was found at all sites studied. What is different in the
494 specific events is the lack or very slow growth during the daytime. Lower temperature (-0.81°C),
495 incoming solar radiation (112 Wm^{-2}) and higher relative humidity (68.4%) occurred on event days
496 with later growth, while no clear wind association was found. Lower concentrations of organic
497 matter and nitrate were found throughout the days with later growth compared to the rest of the
498 NPF days. The very high average particle number concentration in the smaller size bins is due to
499 particles, though not growing to larger sizes for some time, persisting in the local atmosphere for
500 hours. These results though should be used with caution due to the limited number of observations.
501

502 3.3.4 Spain

503 The atmospheric conditions favouring NPF events at both sites are similar to most other sites,
504 though with lower wind speed on event days compared to the average conditions ($p < 0.001$ at
505 SPAUB). The wind profile between the two sites is different, with mainly northwesterly and
506 southeasterly winds for SPARU (which seems to be affected by the local topography), while a more
507 balanced profile is found at SPAUB. For both sites, though, increased probability for NPF events is
508 found for westerly and northwesterly winds. These incoming wind directions originate from a rather
509 clean area with low concentrations of pollutants and condensation sink. At SPARU, incoming wind
510 from directions with higher concentrations of pollutants and condensation sink were associated with
511 lower frequency of NPF events but higher growth rates. At SPAUB, NPF events were relatively
512 rare and growth rates were lower with easterly wind directions, as air masses originating from that
513 section have passed from the city centre and the industrial areas from the Besos River. Due to this,
514 incoming air masses from these sectors had higher concentrations of pollutants and condensation
515 sink.

516

517 While NPF events with subsequent growth of the particles were rare during summer, cases of bursts
518 of particles in the smallest size range available were found to occur frequently, especially in August
519 and July (the month with the fewest NPF events, despite the favourable meteorological conditions).
520 In such cases, a new mode of particles appears in the smallest size available, persisting for many
521 hours though without clear growth (brief or no growth is only observed), as reported by Dall'Osto

522 et al. (2012). Due to the lack of growth of the particles these burst events do not qualify as NPF
523 events using the criteria set in the present study. These burst events are associated with southerly
524 winds (known as Garbí-southwest and Migjorn-south in Catalan, which are common during the
525 summer in the area) that bring a large number of particles smaller than 30 nm to the site from the
526 nearby airport (located about 15 km to the southwest) and port (7 km south), as well as Saharan
527 dust, increasing the concentrations of PM (Rodríguez et al., 2001) and thus suppressing NPF events
528 due to the increased condensation sink.

529

530 Finally, the wind direction profile at SPARU appears to have a daily trend, with almost exclusively
531 stronger southeasterly winds at about midday (Figure S3), probably due to a local mesoscale
532 circulation caused by the increased solar activity during that time (which results in different heating
533 patterns of the various land types in the greater area). These incoming southeast winds are more
534 polluted and have a higher condensation sink (being affected by the city of Barcelona), and almost
535 consistently bring larger particles at the site during the midday period. This may explain to an
536 extent the lowest probability for NPF events from that sector, despite the very high concentrations
537 of O₃ associated with them, with some extreme values well above 100 µg m⁻³ (Querol et al., 2017).
538 The highest average growth rates are also found from that direction.

539

540

541

542 3.3.5 Greece

543 Temperature and wind speed are found to be lower on NPF event days at the Greek sites, though the
544 differences are minimal and are associated with the seasonal variability of the events. The wind rose
545 in GREUB mainly consists of northeasterly and southwesterly winds. Due to its position, the site is
546 heavily affected by emissions in Athens city centre with westerly winds, resulting in increased
547 particle number concentrations and condensation sink. Despite this, the highest NPF probability and
548 growth rates were found with a northwesterly wind directions. This may be due to them being
549 associated with the highest solar radiation (probably the result of seasonal and diurnal variation),
550 temperature and the lowest relative humidity, along with the highest condensation sink and particle
551 number concentrations of almost all sizes. Chemical composition data was not available for
552 GREUB, though SO₂ concentrations are rather low in Athens and kept declining after the economic
553 crisis (Vrekoussis et al., 2013). The seasonality of SO₂ concentration in Athens favoured winter
554 months and was at its lowest during summer for the period studied (YIIEKA, 2012) (this trend
555 changed later as SO₂ concentrations further declined), which may also be a factor in the seasonality
556 of NPF events, though this will be further discussed later.

557

558 At the GRERU site, the wind profile is mainly westerly, and though it coincides with the most
559 important source of pollutants in the area, the city of Herakleio, its effect while observable is not
560 significant due to the topography in the area. The wind profile for NPF events is similar to the
561 average with significantly higher wind speeds ($p < 0.001$). In general, GRERU has very low

562 pollutant concentrations, with an average NO of $0.073 \mu\text{g m}^{-3}$, NO₂ of $0.52 \mu\text{g m}^{-3}$ and SO₂ in
563 concentrations below 1 ppb (Kouvarakis et al., 2002). Due to this, the differences in the chemical
564 composition in the atmosphere are also minimal. For the specific site two different patterns of
565 development of NPF events were found. In one case, NPF events occurred in a rather clear
566 background, while in the other one they were accompanied with an increase in number
567 concentrations of larger particles or a new mode appearing at larger sizes (about a third of the
568 events). No differences were found in the seasonal variation between the two groups; increased
569 gaseous pollutant and particulate organic carbon concentrations were found for the second group
570 (though the differences were rather small) and a wind rose that favoured southwesterly winds
571 (originating from mainland Crete) instead of the northwesterly (originating from the sea) ones for
572 the first group. The growth rate for the two groups was found to be 3.56 nm h^{-1} for the first group
573 and 4.17 nm h^{-1} for the second, which might be due to the increased presence of condensable
574 compounds. As the dataset starts from the particle size of 8.77 nm, the possibility that these
575 particles were advected from nearby areas should not be overlooked, though they persisted and
576 grew at the site. Other than that, no significant differences were found for the different wind
577 directions.

578

579 As mentioned earlier, both sites had a very low frequency of events and J₁₀ in summer similar to
580 previous studies also reporting few or no events during summer (Vratolis et al., 2019; Ždímal et al.,
581 2011), though the incoming solar radiation is the highest and relative humidity is the lowest during

582 that season. This variation was also observed by Kalivitis et al. (2012) who associated the seasonal
583 variation of NPF events at GRERU with the concentrations of atmospheric ions. The effect of the
584 Etesian winds (known as Meltemia in Greek), which dominate the southern Aegean region during
585 the summer months though should not be overlooked. These result in very strong winds with an
586 average wind speed of 8.15 m s^{-1} during summer at the Finokalia site, and increased turbulence
587 found in all years with available data, affecting both sites of this study. During this period, $N_{<30\text{nm}}$
588 drops to half or less compared to other seasons at both sites, while $N_{>100\text{nm}}$ is at its maximum due to
589 particle aging (Kalkavouras et al., 2017), increasing the condensation sink, especially in GRERU
590 (the effect in GREUB is less visible due to both the wind profile, blowing from east which is a less
591 polluted area, as well as the reduction of urban activities during summer months in Athens). Both
592 the increased condensation sink and turbulence are possible factors for the reduced number of NPF
593 events found at both sites in summer. Another possible factor is the effect of high temperatures in
594 destabilising the molecular clusters critical to new particle formation.

595

596 **3.4 Region-Wide Events**

597 Region-wide events are NPF events which occur over large-scale areas, that may cover hundreds of
598 kilometres (Shen et al., 2018). In the present study, NPF events that took place on the same day at
599 both background sites (urban background and rural) are considered as regional and their conditions
600 are studied (Table S8). The background sites in Greece were not considered due to the great
601 distance between them (about 350 km). There is also uncertainty for the background sites in

602 Finland, where the distance is about 190 km, though a large number of days were found when NPF
603 events occurred on the same day. The number of region-wide events per season (or the fraction of
604 region-wide events to total NPF events) is found in Figure 8 and it appears as if they are more
605 probable in spring at all the sites of the present study (apart from Finland, though the number of
606 events in winter was low), despite the differences found in absolute numbers.

607

608 In Denmark, about 20% of NPF events in DENRU were regional (the percentage is higher for
609 DENUB due to the smaller number of events, at 29%). The relatively low frequency of region-wide
610 NPF events can be explained by the different seasonal dependence of NPF events (region-wide NPF
611 events were more frequent in spring compared to the average due to the seasonality of NPF events
612 in DENUB). Compared to local NPF event conditions, higher wind speed and solar radiation, as
613 well as O₃ and marine compound concentrations (results not included) were found, while the
614 concentrations of all pollutants (such as NO, NO_x, sulphate, elemental and organic carbon) were
615 lower. These cleaner atmospheric conditions are also confirmed by the lower CS associated with
616 region-wide events, which is probably one of the most important factors in the occurrence of these
617 large-scale events. The exceptions found at DENRU (increased relative humidity and less incoming
618 solar radiation) are probably due to the different seasonality between local and region-wide NPF
619 events at the site, though region-wide events rarely present similar characteristics at different sites
620 even in the same country due to the differences in the initial meteorological and local conditions
621 (Hussein et al., 2009). The growth rates of region-wide events were found to be lower than those of

622 local events at both sites, which is probably associated with the limited concentrations of
623 condensable compounds due to the cleaner air masses of marine origin (as confirmed by the higher
624 concentrations of marine compounds).

625
626 In Germany, the majority of NPF events of this study were region-wide (about 60%). Compared to
627 the average, the meteorological conditions found for NPF event days compared to average
628 conditions were more distinct for the region-wide events, with even lower wind speed and relative
629 humidity and higher temperature and solar radiation, and all of these differences were significant (p
630 < 0.001). At GERRU where chemical composition data was available, higher concentrations of
631 particulate organic carbon and sulphate and lower nitrate concentrations were found. The
632 differences are significant ($p < 0.001$) and may explain the higher growth rates found in region-wide
633 events at both sites compared to the average, which is a unique feature. It should be noted that as
634 the majority of NPF events at the German sites are associated with easterly winds, it is expected that
635 in most cases the region-wide events will be associated with these, carrying the characteristics that
636 come along with them (increased growth rates and concentrations of organic carbon, as discussed in
637 Section 3.2).

638
639 In Finland, about a quarter of the NPF event days at FINRU (26%) occurred on the same day as at
640 FINUB (the frequency is a lot higher for FINUB, at 39%). As in Germany, the meteorological
641 conditions found on NPF event days compared to average conditions were more distinct during

642 region-wide events. Thus, for both sites temperature and relative humidity were lower while solar
643 radiation was higher. The different trend found for the wind speed at the two sites (being higher on
644 average NPF days at FINRU and lower at FINUB compared to average conditions) was enhanced
645 as well at the two sites for region-wide events. At FINRU where chemical composition data was
646 available, NO_x and SO₂ had similar concentrations on region-wide event days compared to the
647 averages on total event days, while O₃ was significantly higher ($p < 0.001$). As at most other sites,
648 the growth rate was found lower on region-wide event days compared to the average at both sites.

649

650 Finally, in Spain the datasets of the two sites did not overlap greatly, having only 322 common
651 days. Among these days, 13 days presented with NPF events that took place simultaneously at both
652 sites, with smaller growth rates on average compared to local events (43% of the events at SPARU
653 and 36% of the events at SPAUB in the period 8/2012 to 1/2013 and 2014 when data for both sites
654 were available). Due to the small number of common events the results are quite mixed with the
655 only consistent result being the lower relative humidity and higher O₃ concentrations for regional
656 events at both sites, though none of these differences is significant. The wind profile at SPAUB
657 seems to further favour the cleaner sector, with the majority of incoming winds being from the NW
658 and even higher wind speeds (though with low significance). The result is similar at SPARU,
659 though less clear and with lower wind speeds.

660

661 These results are in general in agreement with those found in the UK in a previous study, where
662 meteorological conditions were more distinct on region-wide event days compared to local NPF
663 events; pollutant concentrations were lower as well as the growth rates of the newly formed
664 particles (Bousiotis et al., 2019).

665
666 Common events were also found between either of the background sites and the roadside, but they
667 were always fewer in number, due to the difference in their temporal variability compared to the
668 background sites, resulting from the effect of roadside pollution.

669

670 **3.5 The Effect of NPF Events on the Ultrafine Particle Concentrations**

671 The NSF is a metric of the effect of NPF events upon particle concentrations on either the days of
672 the events or over a larger timescale. Both the NSF_{NUC} and NSF_{GEN} were calculated for all sites of
673 this study and the results are presented in Figure 9. For almost all rural background sites NSF_{NUC} ,
674 which indicates the effect of NPF on ultrafine particle concentrations on the day of the event, was
675 found to be greater than 2 (the only exception was GERRU), which means that NPF events more
676 than double the number of ultrafine particles (particles with diameter smaller than 100 nm) at the
677 site on the days of the events, as NPF events are one of the main sources of ultrafine particles in this
678 type of sites, especially below 30 nm. This reaches up to 4.18 found at FINRU (418% more
679 ultrafine particles on the day of the events – 100% being the average), showing the great effect NPF
680 events have on rather clean areas. The long-term effect was smaller, and it was found that at FINRU

681 NPF events increase the number of ultrafine particles by an additional 130% in general. The effect
682 of NPF events was a lot smaller at the urban sites, though still significant at urban background sites
683 (reaching up 240% at FINUB on the days of events), while roadsides had the smallest NSF
684 compared to their respective background sites. This is because of the increased effect of local
685 sources such as traffic or heating, and the associated increased condensation sink found within these
686 sites, which cause the new particles to be scavenged by the more polluted background.

687

688 The calculation of NSF at the sites around Europe showed a weakness of the specific metric, which
689 points to the need for more careful interpretation of the results of this metric, especially at roadside
690 sites. At FINRO, the NSF_{NUC} provided a value smaller than 1, which translates as ultrafine particles
691 are lost instead of formed on NPF event days. This though is the result of both the sharp reduction
692 in particle number concentrations at all modes that are required for NPF events to occur at a busy
693 roadside (much lower condensation sink), as well as a difference in the ratio between smaller to
694 larger particles (smaller or larger than 100 nm) on NPF event days (favouring the larger particles) at
695 the specific site. Similarly, the long-term effect of NPF events at the site was found to be 1, which
696 means that NPF events appear to cause no changes in the number concentration of ultrafine
697 particles.

698

699

700

701 4. DISCUSSION

702 4.1 Variability of the Frequency and Seasonality of the Events

703 ~~The most consistent result found throughout the areas studied, regardless of the geographical~~
704 ~~location was the~~ higher frequency of NPF events at the rural background sites compared to
705 roadsides was found for all countries with available data for both types of site. This pattern comes
706 in contrast with what was found for the more polluted Asian cities (Peng et al., 2017; Wang et al.,
707 2017), where NPF events were more frequent at the urban sites. This is probably associated with the
708 even greater abundance of condensable species (which further enhances the growth of the particles,
709 thus increasing their chance of survival), deriving from anthropogenic emissions, found in Asian
710 megacities compared to European ones and results in a greater frequency of NPF events in Asian
711 cities, even compared to the most polluted cities in Europe. This contrast emphasises the differences
712 in the occurrence of NPF events between the polluted cities in Europe and Asia, which are
713 associated with the level of pollution found in them, as well as the influence that the level of
714 pollution has on the occurrence of NPF events in general.

715

716 The type of site dependence found in Europe together with the average conditions found on NPF
717 event days compared to the average for each site, underline the importance of clear atmospheric
718 conditions (high solar radiation and low relative humidity and pollutant concentrations) at all types
719 of sites in Europe, especially for region-wide events. The temperature and wind speed presented
720 more diverse results which in many cases are associated with local conditions. The origin of the

721 incoming air masses though, appears to have a more important influence upon the NPF events.
722 Cleaner air masses tend to have higher probability for NPF events, a result which was consistent
723 among the sites of this study regardless of their type.

724

725 The frequency of NPF events at roadsides peaked in summer in all three countries with available
726 data. Greater variability in the seasonality of NPF events was found at the background sites. The
727 urban background sites presented more diverse results, for both the occurrence and development of
728 NPF events, especially compared to rural background sites. The within-week variation of NPF
729 events was found to favour weekends in most cases, as the pollution levels decrease, due to the
730 weekly cycle, especially at the roadsides. As background sites have smaller variations between
731 weekdays and weekends, the within-week variation of NPF events is smaller at the urban
732 background sites and almost non-existent at the rural background sites. Finally, it should be noted
733 that no clear interannual trend was found in the frequency of the events for any site, even for those
734 with longer datasets.

735

736 **4.2 Variability and Seasonality of the Formation and Growth Rate**

737 The growth rate of the newly formed particles was found to be higher at all the roadsides compared
738 to their respective rural and urban background. The picture is similar for J_{10} , (the rate of formed
739 particles associated with NPF events that reached 10 nm diameter), for which urban background
740 sites were between their respective rural background sites and the roadsides with the sole exception

741 of DENUB (the difference with DENRU is rather small though). The growth and formation rate at
742 the rural background sites (apart from the Greek site) were found to be higher in summer compared
743 to the other seasons. On the other hand, the seasonality of the growth rate at the roadsides is not
744 clear but the formation rate peaks in the autumn at all three roadside sites. While the trend at the
745 rural sites is probably associated with the enhanced photochemistry and increased concentrations of
746 BVOCs during summer, the seasonality of the growth rate at the roadside sites is more difficult to
747 explain and probably shows the smaller importance of the BVOCs compared to the compounds of
748 anthropogenic origin (which are in less abundance in summer) in this type of environment. In
749 general, higher temperatures were associated with higher growth rates. This though applies only for
750 the specific conditions at each site and cannot be used as a general rule for the expected growth rate
751 at a site, as locations with higher temperatures did not present higher growth rates. Additionally, the
752 origin of the incoming air masses appears to have an effect on the growth of the particles as well. In
753 most of the sites in this study, incoming air masses from directions associated with higher
754 concentrations of pollutants presented higher growth rates of the newly formed particles. The effect
755 of the different wind directions upon the formation rate was more complex and a definitive
756 conclusion cannot be made. Finally, as with the frequency of the events, no significant interannual
757 trend was found in the variation of the formation or the growth rate across the sites studied.

758

759

760

761 **4.3 Effect of Local Conditions in the Occurrence and Development of NPF Events**

762 Apart from the general meteorological and atmospheric conditions that affect the occurrence and
763 the metrics of NPF events, conditions with a more local character were found to play a significant
764 role as well. These include synoptic systems, such as the one occurring during the summer at the
765 Greek sites, affecting the frequency and seasonality of the events. As a result, sites or seasons with
766 conditions that favoured NPF presented decreased frequency of events and unexpected seasonality,
767 due to the increased turbulence caused by such pressure systems. Additionally, local sources of
768 pollution can also have a significant impact in the temporal trends and metrics of the events, even
769 for sites of very close proximity. One such example was the urban sites in Denmark, which despite
770 being affected by the same source of pollution (the nearby port) and being only a few kilometres
771 away from each other, presented different outcomes in the occurrence of the events. This was due to
772 the different atmospheric composition found between them, being a background and a roadside site,
773 which led to a different response in that local variable. In this case, the effect of the specific source
774 was more prominent at the urban background site compared to the roadside, resulting in fewer NPF
775 events, as the newly formed particles were more effectively suppressed at the urban background site,
776 due to their slower growth.

777

778 **5. CONCLUSIONS**

779 There are different ways to assess the occurrence of new particle formation (NPF) events. In this
780 study, the frequency of NPF events, the formation and growth rate of the particles associated with

781 secondary formation of particles and not primary emissions, at 13 sites from five countries in
782 Europe are considered. NPF is a complicated process, affected by many meteorological and
783 environmental variables. The seasonality of these variables, which varies throughout Europe, results
784 in the different temporal trends found for the metrics studied in this paper. Apart from
785 meteorological conditions though, some of which have a uniform effect (such as the solar radiation
786 intensity and relative humidity), many local variables can also have a positive or negative effect in
787 the occurrence of these events. Sites with less anthropogenic influence seem to have temporal
788 trends dependant on the seasonality of synoptic conditions and general atmospheric composition.
789 The urban sites though and especially those with significant sources of pollution in close proximity,
790 present more complex trends as the NPF occurrence depends less upon favourable meteorological
791 conditions and more upon the local atmospheric conditions, including composition. As NPF event
792 occurrence is based on the balance between the rapid growth of the newly formed particles and their
793 loss from processes, such as the evaporation or coagulation of the particles, the importance of
794 significant particle formation, fast growth (which is enhanced by the increased presence of
795 condensable compounds from anthropogenic activities found in urban environments) and low
796 condensation sink is increased within such environments, also affecting the temporal trends of the
797 events, making them more probable during periods with smaller pollution loads (e.g. summer,
798 weekends). This explains the smaller frequency of NPF events at roadside sites compared to their
799 respective background sites, despite the greater formation and growth rates observed in them.
800 Consequently, NPF events have a smaller influence on the ultrafine particle load at the urban sites

801 compared to background sites, due to both the increased presence of ultrafine particles from
802 anthropogenic emissions as well as the smaller probability of ultrafine particles to survive in such
803 environments.

804

805 Nevertheless, NPF events are an important source of ultrafine particles in the atmosphere for all
806 types of environment and are an important factor in the air quality of a given area. The present
807 study underlines the importance of both the synoptic and local conditions on NPF events, the mix of
808 which not only affects their development but can also influence their occurrence even in areas of
809 very close proximity. NPF is a complex process, affected by numerous variables, making it
810 extremely difficult to predict any of its metrics without considering multiple factors. Since the
811 mechanisms and general trends in NPF events are yet to be fully explained and understood, more
812 laboratory and field studies are needed to generate greater clarity and predictive capability.

813

814 **DATA ACCESSIBILITY**

815 Data supporting this publication are openly available from the UBIRA eData repository at
816 <https://doi.org/10.25500/edata.bham.00000467>

817

818 **AUTHOR CONTRIBUTIONS**

819 The study was conceived and planned by MDO and RMH who also contributed to the final
820 manuscript. The data analysis was carried out by DB who also prepared the first draft of the

821 manuscript. AM, JKN, CN, JVN, HP, NP, AA, GK, SV and KE have provided with the data for the
822 analysis. FDP, XQ, DCB and TP provided advice on the analysis.

823

824 **COMPETING INTERESTS**

825 The authors have no conflict of interests.

826

827 **ACKNOWLEDGMENTS**

828 This work was supported by the National Centre for Atmospheric Science funded by the U.K.

829 Natural Environment Research Council (R8/H12/83/011).

830 **REFERENCES**

831

832 Aalto, P., Hämeri, K., Becker, E. D. O., Weber, R., Salm, J., Mäkelä, J. M., Hoell, C., O'Dowd, C.
833 D., Karlsson, H., Hansson, H., Väkevä, M., Koponen, I. K., Buzorius, G. and Kulmala, M.: Physical
834 characterization of aerosol particles during nucleation events, *Tellus, Ser. B Chem. Phys. Meteorol.*,
835 53(4), 344–358, doi:10.3402/tellusb.v53i4.17127, 2001.

836

837 Alam, A., Shi, J. P. and Harrison, R. M.: Observations of new particle formation in urban air, *J.*
838 *Geophys. Res. Atmos.*, 108(D3), 4093, doi:10.1029/2001JD001417, 2003.

839

840 Atkinson, R. W., Fuller, G. W., Anderson, H. R., Harrison, R. M. and Armstrong, B.: Urban
841 ambient particle metrics and health: A time-series analysis, *Epidemiology*, 21(4), 501–511,
842 doi:10.1097/EDE.0b013e3181debc88, 2010.

843

844 Bianchi, F., Kurtén, T., Riva, M., Mohr, C., Rissanen, M. P., Roldin, P., Berndt, T., Crouse, J. D.,
845 Wennberg, P. O., Mentel, T. F., Wildt, J., Junninen, H., Jokinen, T., Kulmala, M., Worsnop, D. R.,
846 Thornton, J. A., Donahue, N., Kjaergaard, H. G. and Ehn, M.: Highly oxygenated organic
847 molecules (HOM) from gas-phase autoxidation involving peroxy radicals : A key contributor to
848 atmospheric aerosol, *Chem. Rev.*, 119, 3472–3509, doi:10.1021/acs.chemrev.8b00395, 2019.

849

850 Birmili, W., Weinhold, K., Rasch, F., Sonntag, A., Sun, J., Merkel, M., Wiedensohler, A., Bastian,
851 S., Schladitz, A., Löschau, G., Cyrys, J., Pitz, M., Gu, J., Kusch, T., Flentje, H., Quass, U.,
852 Kaminski, H., Kuhlbusch, T. A. J., Meinhardt, F., Schwerin, A., Bath, O., Ries, L., Wirtz, K. and
853 Fiebig, M.: Long-term observations of tropospheric particle number size distributions and
854 equivalent black carbon mass concentrations in the German Ultrafine Aerosol Network (GUAN),
855 *Earth Syst. Sci. Data*, 8(2), 355–382, doi:10.5194/essd-8-355-2016, 2016.

856

857 Bousiotis, D., Osto, M. D., Beddows, D. C. S., Pope, F. D., Harrison, R. M. and Harrison, C. R. M.:
858 Analysis of new particle formation (NPF) events at nearby rural , urban background and urban
859 roadside sites, 19, 5679–5694, 2019.

860

861 Boy, M., Kulmala, M., Ruuskanen, T. M., Pihlatie, M., Reissell, A., Aalto, P. P., Keronen, P., Dal
862 Maso, M., Hellen, H., Hakola, H., Jansson, R., Hanke, M. and Arnold, F.: Sulphuric acid closure
863 and contribution to nucleation mode particle growth, *Atmos. Chem. Phys.*, 5(4), 863–878,
864 doi:10.5194/acp-5-863-2005, 2005.

865

866 Brean, J., Harrison, R. M., Shi, Z., Beddows, D. C. S., Acton, W. J. F. and Hewitt, C. N.:
867 Observations of highly oxidised molecules and particle nucleation in the atmosphere of Beijing,
868 *Atmos. Chem. Phys.*, 19, 14933–14947, 2019, doi.org/10.5194/acp-19-14933-2019, 2019.

869

870 Brines, M., Dall'Osto, M., Beddows, D. C. S., Harrison, R. M., Gómez-Moreno, F., Núñez, L.,
871 Artíñano, B., Costabile, F., Gobbi, G. P., Salimi, F., Morawska, L., Sioutas, C. and Querol, X.:
872 Traffic and nucleation events as main sources of ultrafine particles in high-insolation developed
873 world cities, *Atmos. Chem. Phys.*, 15(10), 5929–5945, doi:10.5194/acp-15-5929-2015, 2015.
874

875 Brines, M., Dall'Osto, M., Beddows, D. C. S., Harrison, R. M. and Querol, X.: Simplifying aerosol
876 size distributions modes simultaneously detected at four monitoring sites during SAPUSS, *Atmos.*
877 *Chem. Phys.*, 14(6), 2973–2986, doi:10.5194/acp-14-2973-2014, 2014.
878

879 Carnerero, C., Pérez, N., Reche, C., Ealo, M., Titos, G., Lee, H., Eun, R., Park, Y., Dada, L.,
880 Paasonen, P., Kerminen, V., Mantilla, E., Escudero, M., Gómez-moreno, F. J., Alonso-blanco, E.,
881 Coz, E., Saiz-, A., Temime-roussel, B., Marchand, N., Beddows, D. C. S. and Harrison, R. M.:
882 Vertical and horizontal distribution of regional new particle formation events in Madrid, *Atmos.*
883 *Chem. Phys.*, 1–27, doi:10.5194/acp-2018-173, 2018.
884

885 Charron, A., Birmili, W. and Harrison, R. M.: Fingerprinting particle origins according to their size
886 distribution at a UK rural site, *J. Geophys. Res. Atmos.*, 113(7), 1–15, doi:10.1029/2007JD008562,
887 2008.
888

889 Cheung, H. C., Chou, C. C.-K., Huang, W.-R. and Tsai, C.-Y.: Characterization of ultrafine particle
890 number concentration and new particle formation in an urban environment of Taipei, Taiwan,
891 *Atmos. Chem. Phys.*, 13(17), 8935–8946, doi:10.5194/acp-13-8935-2013, 2013.
892

893 Chu, B., Kerminen, V., Bianchi, F., Yan, C., Petäjä, T. and Kulmala, M.: Atmospheric new particle
894 formation in China, *Atmos. Chem. Phys.*, 19, 115–138, doi.org/10.5194/acp-19-115-2019, 2019.
895

896 Costabile, F., Birmili, W., Klose, S., Tuch, T., Wehner, B., Wiedensohler, A., Franck, U., König, K.
897 and Sonntag, A.: Spatio-temporal variability and principal components of the particle number size
898 distribution in an urban atmosphere, *Atmos. Chem. Phys.*, 9(9), 3163–3195, doi:10.5194/acp-9-
899 3163-2009, 2009.
900

901 Dal Maso, M., Kulmala, M., Riipinen, I., Wagner, R., Hussein, T., Aalto, P. P. and Lehtinen, K. E.
902 J.: Formation and growth of fresh atmospheric aerosols: Eight years of aerosol size distribution data
903 from SMEAR II, Hyytiälä, Finland, *Boreal Environ. Res.*, 10(5), 323–336,
904 doi:10.1016/j.ijpharm.2012.03.044, 2005.
905

906 Dal Maso, M., Kulmala, M., Lehtinen, K. E. J., Mäkelä, J. M., Aalto, P. and O'Dowd, C. D.:
907 Condensation and coagulation sinks and formation of nucleation mode particles in coastal and
908 boreal forest boundary layers, *J. Geophys. Res. Atmos.*, 107(19), doi:10.1029/2001JD001053, 2002.
909

910 Dall'Osto, M., Beddows, D. C. S., Asmi, A., Poulain, L., Hao, L., Freney, E., Allan, J. D.,
911 Canagaratna, M., Crippa, M., Bianchi, F., De Leeuw, G., Eriksson, A., Swietlicki, E., Hansson, H.
912 C., Henzing, J. S., Granier, C., Zemankova, K., Laj, P., Onasch, T., Prevot, A., Putaud, J. P.,
913 Sellegri, K., Vidal, M., Virtanen, A., Simo, R., Worsnop, D., O'Dowd, C., Kulmala, M. and
914 Harrison, R. M.: Novel insights on new particle formation derived from a pan-european observing
915 system, *Sci. Rep.*, 8(1), 1–11, doi:10.1038/s41598-017-17343-9, 2018.

916
917 Dall'Osto, M., Querol, X., Alastuey, A., O'Dowd, C., Harrison, R. M., Wenger, J. and Gómez-
918 Moreno, F. J.: On the spatial distribution and evolution of ultrafine particles in Barcelona, *Atmos.*
919 *Chem. Phys.*, 13(2), 741–759, doi:10.5194/acp-13-741-2013, 2013.

920
921 Dall'Osto, M., Beddows, D. C. S., Pey, J., Rodriguez, S., Alastuey, A., M. Harrison, R. and Querol,
922 X.: Urban aerosol size distributions over the Mediterranean city of Barcelona, NE Spain, *Atmos.*
923 *Chem. Phys.*, 12(22), 10693–10707, doi:10.5194/acp-12-10693-2012, 2012.

924
925 Dameto de España, C., Wonaschütz, A., Steiner, G., Rosati, B., Demattio, A., Schuh, H. and
926 Hitznerberger, R.: Long-term quantitative field study of New Particle Formation (NPF) events as a
927 source of Cloud Condensation Nuclei (CCN) in the urban background of Vienna, *Atmos. Environ.*,
928 164, 289–298, doi:10.1016/j.atmosenv.2017.06.001, 2017.

929
930 Deng C., Fu, F., Dada, L., Yan, C., Cai, R., Yang, D., Zhou, Y., Yin, R., Lu, Y., Li, X., Fan, X.,
931 Nie, W., Kontkanen, J., Kangasluoma, J., Chu, B., Ding, A., Kerminen, V.-M., Paasonen, P.,
932 Worsnop, D.R., Bianchi, F., Liu, Y., Zheng, J., Wang, L., Kulmala, M. and Jiang, J.: Seasonal
933 Characteristics of New Particle Formation and Growth in Urban Beijing, *Environ. Sci. Technol.*, 54,
934 8547 – 8557, 2020.

935
936 Ehn, M., Thornton, J. A., Kleist, E., Sipilä, M., Junninen, H., Pullinen, I., Springer, M., Rubach, F.,
937 Tillmann, R., Lee, B., Lopez-Hilfiker, F., Andres, S., Acir, I. H., Rissanen, M., Jokinen, T.,
938 Schobesberger, S., Kangasluoma, J., Kontkanen, J., Nieminen, T., Kurtén, T., Nielsen, L. B.,
939 Jørgensen, S., Kjaergaard, H. G., Canagaratna, M., Maso, M. D., Berndt, T., Petäjä, T., Wahner, A.,
940 Kerminen, V. M., Kulmala, M., Worsnop, D. R., Wildt, J. and Mentel, T. F.: A large source of low-
941 volatility secondary organic aerosol, *Nature*, 506(7489), 476–479, doi:10.1038/nature13032, 2014.

942
943 Fuchs, N. A. and Sutugin, A. G.: Highly dispersed aerosols, *Foreign Sci. Technol. Center*, 1-86,
944 1971.

945
946 Hama, S. M. L., Cordell, R. L., Kos, G. P. A., Weijers, E. P. and Monks, P. S.: Sub-micron particle
947 number size distribution characteristics at two urban locations in Leicester, *Atmos. Res.*, 194, 1–16,
948 doi:10.1016/j.atmosres.2017.04.021, 2017.

949

950 Hao, L., Garmash, O., Ehn, M., Miettinen, P., Massoli, P., Mikkonen, S. and Jokinen, T.: Combined
951 effects of boundary layer dynamics and atmospheric chemistry on aerosol composition during new
952 particle formation periods, *Atmos. Chem. Phys.*, 18, 17705–17716, doi.org/10.5194/acp-18-17705-
953 2018, 2018.

954

955 Harrison, R. M., Shi, J. P., Xi, S., Khan, A., Mark, D., Kinnersley, R. and Yin, J.: Measurement of
956 number, mass and size distribution of particles in the atmosphere, *Philos. Trans. R. Soc. A Math.*
957 *Phys. Eng. Sci.*, 358(1775), 2567–2580, doi:10.1098/rsta.2000.0669, 2000.

958

959 Hietikko, R., Kuuluvainen, H., Harrison, R. M., Portin, H., Timonen, H., Niemi, J. V and Rönkkö,
960 T.: Diurnal variation of nanocluster aerosol concentrations and emission factors in a street canyon,
961 *Atmos. Environ.*, 189, 98–106, doi:10.1016/j.atmosenv.2018.06.031, 2018.

962

963 Hofman, J., Staelens, J., Cordell, R., Stroobants, C., Zikova, N., Hama, S. M. L., Wyche, K. P.,
964 Kos, G. P. A., Van Der Zee, S., Smallbone, K. L., Weijers, E. P., Monks, P. S. and Roekens, E.:
965 Ultrafine particles in four European urban environments: Results from a new continuous long-term
966 monitoring network, *Atmos. Environ.*, 136, 68–81, doi:10.1016/j.atmosenv.2016.04.010, 2016.

967

968 Hussein, T., Junninen, H., Tunved, P., Kristensson, A., Dal Maso, M., Riipinen, I., Aalto, P. P.,
969 Hansson, H. C., Swietlicki, E. and Kulmala, M.: Time span and spatial scale of regional new
970 particle formation events over Finland and Southern Sweden, *Atmos. Chem. Phys.*, 9(14), 4699–
971 4716, doi:10.5194/acp-9-4699-2009, 2009.

972

973 Iida, K., Stolzenburg, M. R., McMurry, P. H. and Smith, J. N.: Estimating nanoparticle growth rates
974 from size-dependent charged fractions: Analysis of new particle formation events in Mexico City, *J.*
975 *Geophys. Res. Atmos.*, 113(5), 1–15, doi:10.1029/2007JD009260, 2008.

976

977 Jaatinen, A., Hamed, A., Joutsensaari, J., Mikkonen, S., Birmili, W., Wehner, B., Spindler, G.,
978 Wiedensohler, A., Decesari, S., Mircea, M., Facchini, M. C., Junninen, H., Kulmala, M., Lehtinen,
979 K. E. J. and Laaksonen, A.: A comparison of new particle formation events in the boundary layer at
980 three different sites in Europe, *Boreal Environ. Res.*, 14(4), 481–498, 2009.

981

982 Järvi, L., Hannuniemi, H., Hussein, T., Junninen, H., Aalto, P., Hillamo, R., Mäkelä, T., Keronen,
983 P. and Siivola, E.: The urban measurement station SMEAR III : Continuous monitoring of air
984 pollution and surface – atmosphere interactions in Helsinki , Finland, *Boreal Environ. Res.*, 14(4),
985 86–109, 2009.

986

987 Jeong, C.-H. H., Evans, G. J., McGuire, M. L., Y.-W. Chang, R., Abbatt, J. P. D. D., Zeromskiene,
988 K., Mozurkewich, M., Li, S.-M. M., Leitch, W. R., Chang, R. Y.-W., Abbatt, J. P. D. D.,
989 Zeromskiene, K., Mozurkewich, M., Li, S.-M. M. and Leitch, W. R.: Particle formation and

990 growth at five rural and urban sites, *Atmos. Chem. Phys.*, 10(16), 7979–7995, doi:10.5194/acp-10-
991 7979-2010, 2010.
992
993 Kalivitis, N., Stavroulas, I., Bougiatioti, A., Kouvarakis, G., Gagné, S., Manninen, H. E., Kulmala,
994 M. and Mihalopoulos, N.: Night-time enhanced atmospheric ion concentrations in the marine
995 boundary layer, *Atmos. Chem. Phys.*, 12(8), 3627–3638, doi:10.5194/acp-12-3627-2012, 2012.
996
997 Kalivitis, N., Kerminen, V.-M., Kulmala, M., Kanakidou, M., Myriokefalitakis, S., Tzitzikalaki, E.,
998 Roldin, P., Kouvarakis, G., Stavroulas, I., Boy, M., Manninen, H. E., Bougiatioti, A., Daskalakis,
999 N., Petäjä, T., Kalkavouras, P. and Mihalopoulos, N.: Formation and growth of atmospheric
1000 nanoparticles in the eastern Mediterranean: Results from long-term measurements and process
1001 simulations, *Atmos. Chem. Phys.*, 19, 2671–2686, doi.org/10.5194/acp-19-2671-2019, 2019.
1002
1003 Kalivitis, N., Kerminen, V. M., Kouvarakis, G., Stavroulas, I., Bougiatioti, A., Nenes, A.,
1004 Manninen, H. E., Petäjä, T., Kulmala, M. and Mihalopoulos, N.: Atmospheric new particle
1005 formation as a source of CCN in the eastern Mediterranean marine boundary layer, *Atmos. Chem.*
1006 *Phys.*, 15(16), 9203–9215, doi:10.5194/acp-15-9203-2015, 2015.
1007
1008 Kalkavouras, P., Bossioli, E., Bezantakos, S., Bougiatioti, A., Kalivitis, N., Stavroulas, I.,
1009 Kouvarakis, G., Protonotariou, A. P., Dandou, A., Biskos, G., Mihalopoulos, N., Nenes, A. and
1010 Tombrou, M.: New particle formation in the southern Aegean Sea during the Etesians: Importance
1011 for CCN production and cloud droplet number, *Atmos. Chem. Phys.*, 17(1), 175–192,
1012 doi:10.5194/acp-17-175-2017, 2017.
1013
1014 Kerminen, V.-M., Chen, X., Vakkari, V., Petäjä, T., Kulmala, M. and Bianchi, F.: Atmospheric new
1015 particle formation and growth: review of field observations, *Environ. Res. Lett*, 13(10), 103003,
1016 doi:10.1088/1748-9326/aadf3c, 2018.
1017
1018 Kerminen, V. M., Lehtinen, K. E. J., Anttila, T. and Kulmala, M.: Dynamics of atmospheric
1019 nucleation mode particles: A timescale analysis, *Tellus, Ser. B Chem. Phys. Meteorol.*, 56(2), 135–
1020 146, doi:10.3402/tellusb.v56i2.16411, 2004.
1021
1022 Kerminen, V. M., Pirjola, L. and Kulmala, M.: How significantly does coagulation scavenging
1023 limit atmospheric particle production?, *J. Geophys. Res. Atmos.*, 106(D20), 24119–24125,
1024 doi:10.1029/2001JD000322, 2001.
1025
1026 Ketzel, M., Wählin, P., Kristensson, A., Swietlicki, E., Berkowicz, R., Nielsen, O. J. and Palmgren,
1027 F.: Particle size distribution and particle mass measurements at urban, near-city and rural level in
1028 the Copenhagen area and Southern Sweden, *Atmos. Chem. Phys.*, 4(1), 5513–5546,
1029 doi:10.5194/acpd-3-5513-2003, 2004.

1030 Korhonen, P., Kulmala, M., Laaksonen, A., Viisanen, Y., Mcgraw, R. and Seinfeld, J. H.: Ternary
1031 nucleation of H₂SO₄, NH₃ and H₂O in the atmosphere, *J. Geophys. Res.*, 104(D21), 26349–26353,
1032 doi.org/10.1029/1999JD900784, 1999.
1033
1034 Kouvarakis, G., Bardouki, H. and Mihalopoulos, N.: Sulfur budget above the Eastern
1035 Mediterranean: Relative contribution of anthropogenic and biogenic sources, *Tellus, Ser. B Chem.*
1036 *Phys. Meteorol.*, 54(3), 201–212, doi:10.3402/tellusb.v54i3.16661, 2002.
1037
1038 Kristensson, A., Dal Maso, M., Swietlicki, E., Hussein, T., Zhou, J., Kerminen, V. M. and Kulmala,
1039 M.: Characterization of new particle formation events at a background site in southern Sweden:
1040 Relation to air mass history, *Tellus, Ser. B Chem. Phys. Meteorol.*, 60 B(3), 330–344, 2008.
1041
1042 Kulmala, M., Kontkanen, J., Junninen, H., Lehtipalo, K., Manninen, H. E., Nieminen, T., Petäjä, T.,
1043 Sipilä, M., Schobesberger, S., Rantala, P., Franchin, A., Jokinen, T., Järvinen, E., Äijälä, M.,
1044 Kangasluoma, J., Hakala, J., Aalto, P. P., Paasonen, P., Mikkilä, J., Vanhanen, J., Aalto, J., Hakola,
1045 H., Makkonen, U., Ruuskanen, T., Mauldin, R. L., Duplissy, J., Vehkamäki, H., Bäck, J., Kulmala,
1046 M., Petäjä, T., Ehn, M., Thornton, J., Sipilä, M., Worsnop, D. R. and Kerminen, V.-M.: Chemistry
1047 of atmospheric nucleation: On the recent advances on precursor characterization and atmospheric
1048 cluster composition in connection with atmospheric new particle formation, *Annu. Rev. Phys.*
1049 *Chem.*, 65(1), 21–37, doi:10.1146/annurev-physchem-040412-110014, 2014.
1050
1051 Kortelainen, A., Riipinen, I., Kurtén, T., Johnston, M. V., Smith, J. N., Ehn, M., Mentel, T. F.,
1052 Lehtinen, K. E. J., Laaksonen, A., Kerminen, V. M. and Worsnop, D. R.: Direct observations of
1053 atmospheric aerosol nucleation, *Science* (80-.), 339(6122), 943–946,
1054 doi:10.1126/science.1227385, 2013.
1055
1056 Kulmala, M., Petäjä, T., Nieminen, T., Sipilä, M., Manninen, H. E., Lehtipalo, K., Dal Maso, M.,
1057 Aalto, P. P., Junninen, H., Paasonen, P., Riipinen, I., Lehtinen, K. E. J., Laaksonen, A. and
1058 Kerminen, V. M.: Measurement of the nucleation of atmospheric aerosol particles, *Nat. Protoc.*,
1059 7(9), 1651–1667, doi:10.1038/nprot.2012.091, 2012.
1060
1061 Kulmala, M., Petäjä, T., Mönkkönen, P., Koponen, I. K., Dal Maso, M., Aalto, P. P., Lehtinen, K.
1062 E. J. and Kerminen, V.-M.: On the growth of nucleation mode particles: source rates of condensable
1063 vapor in polluted and clean environments, *Atmos. Chem. Phys. Discuss.*, 4(5), 6943–6966,
1064 doi:10.5194/acpd-4-6943-2004, 2005.
1065
1066 Kulmala, M., Vehkamäki, H., Petäjä, T., Dal Maso, M., Lauri, A., Kerminen, V. M., Birmili, W.
1067 and McMurry, P. H.: Formation and growth rates of ultrafine atmospheric particles: A review of
1068 observations, *J. Aerosol Sci.*, 35(2), 143–176, doi:10.1016/j.jaerosci.2003.10.003, 2004a.
1069

1070 Kulmala, M., Laakso, L., Lehtinen, K. E. J., Riipinen, I., Dal Maso, M., Anttila, T., Kerminen, V.-
1071 M., Hörrak, U., Vana, M. and Tammet, H.: Initial steps of aerosol growth, *Atmos. Chem. Phys.*
1072 *Discuss.*, 4(5), 5433–5454, doi:10.5194/acpd-4-5433-2004, 2004b.
1073
1074 Kulmala, M., Dal Maso, M., Mäkelä, J. M., Pirjola, L., Väkevä, M., Aalto, P., Miikkulainen, P.,
1075 Hämeri, K. and O’Dowd, C. D.: On the formation, growth and composition of nucleation mode
1076 particles, *Tellus, Ser. B Chem. Phys. Meteorol.*, 53(4), 479–490, doi:10.3402/tellusb.v53i4.16622,
1077 2001.
1078
1079 Kumar, P., Morawska, L., Birmili, W., Paasonen, P., Hu, M., Kulmala, M., Harrison, R. M.,
1080 Norford, L. and Britter, R.: Ultrafine particles in cities, *Environ. Int.*, 66, 1–10,
1081 doi:10.1016/j.envint.2014.01.013, 2014.
1082
1083 Kupiainen, K., Ritola, R., Stojiljkovic, A., Pirjola, L., Malinen, A. and Niemi, J.: Contribution of
1084 mineral dust sources to street side ambient and suspension PM₁₀ samples, *Atmos. Environ.*, 147,
1085 178–189, doi:10.1016/j.atmosenv.2016.09.059, 2016.
1086
1087 Li, X., Chee, S., Hao, J., Abbatt, J. P. D., Jiang, J. and Smith, J. N.: Relative humidity effect on the
1088 formation of highly oxidized molecules and new particles during monoterpene oxidation, *Atmos.*
1089 *Chem. Phys.*, 19(3), 1555–1570, doi:10.5194/acp-19-1555-2019, 2019.
1090
1091 Ma, N. and Birmili, W.: Estimating the contribution of photochemical particle formation to ultrafine
1092 particle number averages in an urban atmosphere, *Sci. Total Environ.*, 512–513, 154–166,
1093 doi:10.1016/j.scitotenv.2015.01.009, 2015.
1094
1095 Makkonen, R., Asmi, A., Kerminen, V. M., Boy, M., Arneth, A., Hari, P. and Kulmala, M.: Air
1096 pollution control and decreasing new particle formation lead to strong climate warming, *Atmos.*
1097 *Chem. Phys.*, 12(3), 1515–1524, doi:10.5194/acp-12-1515-2012, 2012.
1098
1099 Masiol, M., Harrison, R. M., Vu, T. V. and Beddows, D. C. S.: Sources of sub-micrometre particles
1100 near a major international airport, *Atmos. Chem. Phys.*, 17(20), 12379–12403, doi:10.5194/acp-17-
1101 12379-2017, 2017.
1102
1103 McFiggans, G., Mentel, T. F., Wildt, J., Pullinen, I., Kang, S., Kleist, E., Schmitt, S., Springer, M.,
1104 Tillmann, R., Wu, C., Zhao, D., Hallquist, M., Faxon, C., Le Breton, M., Hallquist, Å. M., Simpson,
1105 D., Bergström, R., Jenkin, M. E., Ehn, M., Thornton, J. A., Alfarra, M. R., Bannan, T. J., Percival,
1106 C. J., Priestley, M., Topping, D. and Kiendler-Scharr, A.: Secondary organic aerosol reduced by
1107 mixture of atmospheric vapours, *Nature*, 565(7741), 587–593, doi:10.1038/s41586-018-0871-y,
1108 2019.
1109

1110 Minguillón, M. C., Brines, M., Pérez, N., Reche, C., Pandolfi, M., Fonseca, A. S., Amato, F.,
1111 Alastuey, A., Lyasota, A., Codina, B., Lee, H. K., Eun, H. R., Ahn, K. H. and Querol, X.: New
1112 particle formation at ground level and in the vertical column over the Barcelona area, *Atmos. Res.*,
1113 164–165, 118–130, doi:10.1016/j.atmosres.2015.05.003, 2015.
1114
1115 Napari, I., Noppel, M., Vehkamäki, H. and Kulmala, M.: An improved model for ternary nucleation
1116 of sulfuric acid-ammonia-water, *J. Chem. Phys.*, 116(10), 4221–4227, doi:10.1063/1.1450557,
1117 2002.
1118
1119 Németh, Z. and Salma, I.: Spatial extension of nucleating air masses in the Carpathian Basin,
1120 *Atmos. Chem. Phys.*, 14(16), 8841–8848, doi:10.5194/acp-14-8841-2014, 2014.
1121
1122 Nieminen, T., Asmi, A., Maso, M. D., Aalto, P. P., Keronen, P., Petäjä, T., Kulmala, M. and
1123 Kerminen, V.: Trends in atmospheric new-particle formation : 16 years of observations in a boreal-
1124 forest environment, *Boreal Environ. Res.*, 19, 191–214, 2014.
1125
1126 Nilsson, E. D., Rannik, Ü., Kulmala, M., Buzorius, G. and O’Dowd, C. D.: Effects of continental
1127 boundary layer evolution, convection, turbulence and entrainment, on aerosol formation, *Tellus*,
1128 *Ser. B Chem. Phys. Meteorol.*, 53(4), 441–461, doi:10.3402/tellusb.v53i4.16617, 2001.
1129
1130 Olin, M., Kuuluvainen, H., Aurela, M., Kalliokoski, J., Kuittinen, N., Isotalo, M., Timonen, H. J.,
1131 Niemi, J. V., Rönkkö, T. and Dal Maso, M.: Traffic-originated nanocluster emission exceeds
1132 H₂SO₄-driven photochemical new particle formation in an urban area, *Atmos. Chem. Phys.*, 20(1),
1133 1–13, doi:10.5194/acp-20-1-2020, 2020.
1134
1135 Ortega, I. K., Kurtén, T., Vehkamäki, H. and Kulmala, M.: The role of ammonia in sulfuric acid ion
1136 induced nucleation, *Atmos. Chem. Phys.*, 8(11), 2859–2867, doi:10.5194/acp-8-2859-2008, 2008.
1137
1138 Park, M., Yum, S. S. and Kim, J. H.: Characteristics of submicron aerosol number size distribution
1139 and new particle formation events measured in Seoul, Korea, during 2004–2012, *Asia-Pacific J.*
1140 *Atmos. Sci.*, 51(1), 1–10, doi:10.1007/s13143-014-0055-0, 2015.
1141
1142 Peng, Y., Dong, Y., Li, X., Liu, X., Dai, J., Chen, C., Dong, Z., Du, C. and Wang, Z.: Different
1143 characteristics of new particle formation events at two suburban sites in northern China,
1144 *Atmosphere*, 8, 258, doi:10.3390/atmos8120258, 2017.
1145
1146 Petäjä, T., Mauldin, R. L., Kosciuch, E., McGrath, J., Nieminen, T., Paasonen, P., Boy, M.,
1147 Adamov, A., Kotiaho, T. and Kulmala, M.: Sulfuric acid and OH concentrations in a boreal forest
1148 site, *Atmos. Chem. Phys.*, 9(19), 7435–7448, doi:10.5194/acp-9-7435-2009, 2009.
1149

1150 Poling, B. E., Prausnitz, J. M. and O'Connell, J. P.: The properties of gases and liquids, 5th Ed.,
1151 McGraw-Hill Education, New York, USA, 768 pp., 2001.
1152

1153 Politis, M., Pilinis, C. and Lekkas, T. D.: Ultrafine particles (UFP) and health effects. Dangerous.
1154 Like no other PM? Review and analysis, *Glob. Nest J.*, 10(3), 439–452, 2008.
1155

1156 Querol, X., Gangoiti, G., Mantilla, E., Alastuey, A., Minguillón, M. C., Amato, F., Reche, C.,
1157 Viana, M., Moreno, T., Karanasiou, A., Rivas, I., Pérez, N., Ripoll, A., Brines, M., Ealo, M.,
1158 Pandolfi, M., Lee, H. K., Eun, H. R., Park, Y. H., Escudero, M., Beddows, D., Harrison, R. M.,
1159 Bertrand, A., Marchand, N., Lyasota, A., Codina, B., Olid, M., Udina, M., Jiménez-Esteve, B. B.,
1160 Jiménez-Esteve, B. B., Alonso, L., Millán, M. and Ahn, K. H.: Phenomenology of high-ozone
1161 episodes in NE Spain, *Atmos. Chem. Phys.*, 17(4), 2817–2838, doi:10.5194/acp-17-2817-2017,
1162 2017.
1163

1164 Riccobono, F., Schobesberger, S., Scott, C. E., Dommen, J., Ortega, I. K., Rondo, L., Almeida, J.,
1165 Amorim, A., Bianchi, F., Breitenlechner, M., David, A., Downard, A., Dunne, E. M., Duplissy, J.,
1166 Ehrhart, S., Flagan, R. C., Franchin, A., Hansel, A., Junninen, H., Kajos, M., Keskinen, H., Kupc,
1167 A., Makhmutov, V., Mathot, S., Nieminen, T., Onnela, A., Petäjä, T., Tsagkogeorgas, G.,
1168 Vaattovaara, P., Viisanen, Y., Vrtala, A. and Wagner, P. E.: Oxidation Products of Biogenic
1169 Atmospheric Particles, *Science*, 717, 717–722, doi:10.1126/science.1243527, 2014.
1170

1171 Riipinen, I., Sihto, S.-L. L., Kulmala, M., Arnold, F., Dal Maso, M., Birmili, W., Saarnio, K.,
1172 Teinilä, K., Kerminen, V.-M. M., Laaksonen, A. and Lehtinen, K. E. J. J.: Connections between
1173 atmospheric sulphuric acid and new particle formation during QUEST III–IV campaigns in
1174 Heidelberg and Hyytiälä, *Atmos. Chem. Phys. Atmos. Chem. Phys.*, 7(8), 1899–1914,
1175 doi:10.5194/acp-7-1899-2007, 2007.
1176

1177 Rimnácová, D., Ždímal, V., Schwarz, J., Smolík, J. and Rimnác, M.: Atmospheric aerosols in
1178 suburb of Prague: The dynamics of particle size distributions, *Atmos. Res.*, 101(3), 539–552,
1179 doi:10.1016/j.atmosres.2010.10.024, 2011.
1180

1181 Rivas, I., Beddows, D. C. S., Amato, F., Green, D. C., Järvi, L., Hueglin, C., Reche, C., Timonen,
1182 H., Fuller, G. W., Niemi, J. V., Pérez, N., Aurela, M., Hopke, P. K., Alastuey, A., Kulmala, M.,
1183 Harrison, R. M., Querol, X. and Kelly, F. J.: Source apportionment of particle number size
1184 distribution in urban background and traffic stations in four European cities, *Environ. Int.*, 135,
1185 105345, doi:10.1016/j.envint.2019.105345, 2020.
1186

1187 Rodríguez, S., Querol, X., Alastuey, A., Kallos, G. and Kakaliagou, O.: Saharan dust contributions
1188 to PM10 and TSP levels in Southern and Eastern Spain, *Atmos. Environ.*, 35(14), 2433–2447,
1189 doi:10.1016/S1352-2310(00)00496-9, 2001.

1190 Rönkkö, T., Kuuluvainen, H., Karjalainen, P., Keskinen, J., Hillamo, R., Niemi, J. V., Pirjola, L.,
1191 Timonen, H. J., Saarikoski, S., Saukko, E., Järvinen, A., Silvennoinen, H., Rostedt, A., Olin, M.,
1192 Yli-Ojanperä, J., Nousiainen, P., Kousa, A. and Dal Maso, M.: Traffic is a major source of
1193 atmospheric nanocluster aerosol, *Proc. Natl. Acad. Sci.*, 114(29), 7549–7554,
1194 doi:10.1073/pnas.1700830114, 2017.
1195
1196 Salma, I., Németh, Z., Kerminen, V. M., Aalto, P., Nieminen, T., Weidinger, T., Molnár, Á., Imre,
1197 K. and Kulmala, M.: Regional effect on urban atmospheric nucleation, *Atmos. Chem. Phys.*, 16(14),
1198 8715–8728, doi:10.5194/acp-16-8715-2016, 2016.
1199
1200 Salma, I., Borsós, T., Németh, Z., Weidinger, T., Aalto, P. and Kulmala, M.: Comparative study of
1201 ultrafine atmospheric aerosol within a city, *Atmos. Environ.*, 92, 154–161,
1202 doi:10.1016/j.atmosenv.2014.04.020, 2014.
1203
1204 Sarnela, N., Jokinen, T., Nieminen, T., Lehtipalo, K., Junninen, H., Kangasluoma, J., Hakala, J.,
1205 Taipale, R., Larnimaa, K., Westerholm, H., Schobesberger, S., Sipil, M., Heijari, J., Kerminen, V.
1206 and Pet, T.: Sulphuric acid and aerosol particle production in the vicinity of an oil refinery, *Atmos.*
1207 *Environ.*, 119, 156–166, doi:10.1016/j.atmosenv.2015.08.033, 2015.
1208
1209 Schobesberger, S., Franchin, A., Bianchi, F., Rondo, L., Duplissy, J., Kürten, A., Ortega, I. K.,
1210 Metzger, A., Schnitzhofer, R., Almeida, J., Amorim, A., Dommen, J., Dunne, E. M., Ehn, M.,
1211 Gagné, S., Ickes, L., Junninen, H., Hansel, A., Kerminen, V. M., Kirkby, J., Kupc, A., Laaksonen,
1212 A., Lehtipalo, K., Mathot, S., Onnela, A., Petäjä, T., Riccobono, F., Santos, F. D., Sipilä, M., Tomé,
1213 A., Tsagkogeorgas, G., Viisanen, Y., Wagner, P. E., Wimmer, D., Curtius, J., Donahue, N. M.,
1214 Baltensperger, U., Kulmala, M. and Worsnop, D. R.: On the composition of ammonia-sulfuric-acid
1215 ion clusters during aerosol particle formation, *Atmos. Chem. Phys.*, 15(1), 55–78, doi:10.5194/acp-
1216 15-55-2015, 2015.
1217
1218 Seinfeld, J. H. and Pandis, S. N.: *Atmospheric Chemistry and Physics: From Air Pollution to*
1219 *Climate Change*, 3rd Editio., John Wiley & Sons, Inc, New Jersey, Canada, 2012.
1220
1221 Shen, X., Sun, J., Kivekäs, N., Kristensson, A., Zhang, X., Zhang, Y., Zhang, L., Fan, R., Qi, X.,
1222 Ma, Q. and Zhou, H.: Spatial distribution and occurrence probability of regional new particle
1223 formation events in eastern China, *Atmos. Chem. Phys.*, 18(2), 587–599, doi:10.5194/acp-18-587-
1224 2018, 2018.
1225
1226 Shi, J. P., Evans, D. E., Khan, A. A. and Harrison, R. M.: Sources and concentration of
1227 nanoparticles (10 nm diameter) in the urban atmosphere, *Atmos. Environ.*, 35, 1193–1202,
1228 doi.org/10.1016/S1352-2310(00)00418-0, 2001.
1229

1230 Siakavaras, D., Samara, C., Petrakakis, M. and Biskos, G.: Nucleation events at a coastal city
1231 during the warm period: Kerbside versus urban background measurements, *Atmos. Environ.*, 140,
1232 60–68, doi:10.1016/j.atmosenv.2016.05.054, 2016.

1233

1234 Sipila, M., Berndt, T., Petaja, T., Brus, D., Vanhanen, J., Stratmann, F., Patokoski, J., Mauldin III,
1235 R. L., Hyvarinen, A. P., Lihavainen, H. and Kulmala, M.: The role of sulfuric acid in atmospheric
1236 nucleation, *Science*, 327, 1243–1246, doi:10.1126/science.1180315, 2010.

1237

1238 Spracklen, D. V., Carslaw, K. S., Kulmala, M., Kerminen, V. M., Sihto, S. L., Riipinen, I.,
1239 Merikanto, J., Mann, G. W., Chipperfield, M. P., Wiedensohler, A., Birmili, W. and Lihavainen, H.:
1240 Contribution of particle formation to global cloud condensation nuclei concentrations, *Geophys.*
1241 *Res. Lett.*, 35(6), 1–5, doi:10.1029/2007GL033038, 2008.

1242

1243 Stanier, C. O., Khlystov, A. Y. and Pandis, S. N.: Nucleation events during the Pittsburgh Air
1244 Quality Study: Description and relation to key meteorological, gas phase, and aerosol parameters,
1245 *Aerosol Sci. Technol.*, 38, 253–264, doi:10.1080/02786820390229570, 2004.

1246

1247 Stojiljkovic, A., Kauhaniemi, M., Kukkonen, J., Kupiainen, K., Karppinen, A., Rolstad Denby, B.,
1248 Kousa, A., Niemi, J. V. and Ketzel, M.: The impact of measures to reduce ambient air PM10
1249 concentrations originating from road dust, evaluated for a street canyon in Helsinki, *Atmos. Chem.*
1250 *Phys.*, 19(17), 11199–11212, doi:10.5194/acp-19-11199-2019, 2019.

1251

1252 Sun, J., Birmili, W., Hermann, M., Tuch, T., Weinhold, K., Spindler, G., Schladitz, A., Bastian, S.,
1253 Löschau, G., Cyrys, J., Gu, J., Flentje, H., Briel, B., Asbach, C., Kaminski, H., Ries, L., Sohmer, R.,
1254 Gerwig, H., Wirtz, K., Meinhardt, F., Schwerin, A., Bath, O., Ma, N., Wiedensohler, A.: Variability
1255 of Black Carbon mass concentrations, sub-micrometer particle number concentrations and size
1256 distributions: Results of the German Ultrafine Aerosol Network ranging from city street to high
1257 Alpine locations, *Atmos. Environ.*, 202, 256-268, 2019.

1258

1259 Tobías, A., Rivas, I., Reche, C., Alastuey, A., Rodríguez, S., Fernández-camacho, R., Sánchez, A.
1260 M., Campa, D., De, J., Sunyer, J. and Querol, X.: Short-term effects of ultra fine particles on daily
1261 mortality by primary vehicle exhaust versus secondary origin in three Spanish cities, *Environ. Int.*,
1262 111, 144–151, doi:10.1016/j.envint.2017.11.015, 2018.

1263

1264 Tröstl, J., Chuang, W. K., Gordon, H., Heinritzi, M., Yan, C., Molteni, U., Ahlm, L., Frege, C.,
1265 Bianchi, F., Wagner, R., Simon, M., Lehtipalo, K., Williamson, C., Craven, J. S., Duplissy, J.,
1266 Adamov, A., Almeida, J., Bernhammer, A. K., Breitenlechner, M., Brilke, S., Dias, A., Ehrhart, S.,
1267 Flagan, R. C., Franchin, A., Fuchs, C., Guida, R., Gysel, M., Hansel, A., Hoyle, C. R., Jokinen, T.,
1268 Junninen, H., Kangasluoma, J., Keskinen, H., Kim, J., Krapf, M., Kürten, A., Laaksonen, A.,
1269 Lawler, M., Leiminger, M., Mathot, S., Möhler, O., Nieminen, T., Onnela, A., Petäjä, T., Piel, F.

1270 M., Miettinen, P., Rissanen, M. P., Rondo, L., Sarnela, N., Schobesberger, S., Sengupta, K., Sipilä,
1271 M., Smith, J. N., Steiner, G., Tomè, A., Virtanen, A., Wagner, A. C., Weingartner, E., Wimmer, D.,
1272 Winkler, P. M., Ye, P., Carslaw, K. S., Curtius, J., Dommen, J., Kirkby, J., Kulmala, M., Riipinen,
1273 I., Worsnop, D. R., Donahue, N. M. and Baltensperger, U.: The role of low-volatility organic
1274 compounds in initial particle growth in the atmosphere, *Nature*, 533(7604), 527–531,
1275 doi:10.1038/nature18271, 2016.
1276
1277 Vassilakos, C., Saraga, D., Maggos, T., Michopoulos, J., Pateraki, S. and Helmis, C. G.: Temporal
1278 variations of PM_{2.5} in the ambient air of a suburban site in Athens, Greece, *Sci. Total Environ.*,
1279 349(1–3), 223–231, doi:10.1016/j.scitotenv.2005.01.012, 2005.
1280
1281 Voigtländer, J., Tuch, T., Birmili, W. and Wiedensohler, A.: Correlation between traffic density and
1282 particle size distribution in a street canyon and the dependence on wind direction, *Atmos. Chem.*
1283 *Phys.*, 6(12), 4275–4286, doi:10.5194/acp-6-4275-2006, 2006.
1284
1285 Vratolis, S., Gini, M. I., Bezantakos, S., Stavroulas, I., Kalivitis, N., Kostenidou, E., Louvaris, E.,
1286 Siakavaras, D., Biskos, G., Mihalopoulos, N., Pandis, S. N. N., Pilinis, C., Papayannis, A. and
1287 Eleftheriadis, K.: Particle number size distribution statistics at City-Centre Urban Background,
1288 urban background, and remote stations in Greece during summer, *Atmos. Environ.*, 213, 711–726,
1289 doi:10.1016/j.atmosenv.2019.05.064, 2019.
1290
1291 Vrekoussis, M., Richter, A., Hilboll, A., Burrows, J. P., Gerasopoulos, E., Lelieveld, J., Barrie, L.,
1292 Zerefos, C. and Mihalopoulos, N.: Economic crisis detected from space: Air quality observations
1293 over Athens/Greece, *Geophys. Res. Lett.*, 40(2), 458–463, doi:10.1002/grl.50118, 2013.
1294
1295 Wang, Z., Wu, Z., Yue, D., Shang, D., Guo, S., Sun, J., Ding, A., Wang, L., Jiang, J., Guo, H., Gao,
1296 J., Cheung, H. C., Morawska, L., Keywood, M. and Hu, M.: New particle formation in China:
1297 Current knowledge and further directions, *Sci. Total Environ.*, 577, 258–266,
1298 doi:10.1016/j.scitotenv.2016.10.177, 2017.
1299
1300 Wang, D., Guo, H., Cheung, K. and Gan, F.: Observation of nucleation mode particle burst and new
1301 particle formation events at an urban site in Hong Kong, *Atmos. Environ.*, 99, 196–205,
1302 doi:10.1016/j.atmosenv.2014.09.074, 2014.
1303
1304 Wang, F., Zhang, Z., Massling, A., Ketzel, M. and Kristensson, A.: Particle formation events
1305 measured at a semirural background site in Denmark, *Environ. Sci. Pollut. Res.*, 20(5), 3050–3059,
1306 doi:10.1007/s11356-012-1184-6, 2013.
1307
1308 Wang, F., Ketzel, M., Ellermann, T., Wählin, P., Jensen, S. S., Fang, D. and Massling, A.: Particle
1309 number, particle mass and NO_x emission factors at a highway and an urban street in Copenhagen,

1310 Atmos. Chem. Phys., 10(6), 2745–2764, doi:10.5194/acp-10-2745-2010, 2010.
1311
1312 Weber, R. J., McMurry, P. H., Mauldin, L., Tanner, D. J., Eisele, F. L., Brechtel, F. J., Kreidenweis,
1313 S. M., Kok, G. L., Schillawski, R. D., Baumgardner, D. and Baumgardner, B.: A study of new
1314 particle formation and growth involving biogenic and trace gas species measured during ACE 1, J.
1315 Geophys. Res. Atmos., 103(D13), 16385–16396, doi:10.1029/97JD02465, 1998.
1316
1317 Weber, R. J., McMurry, P. H., Eisele, F. L. and Tanner, D. J.: Measurement of expected nucleation
1318 precursor species and 3-500-nm diameter particles at Mauna Loa Observatory, Hawaii, J. Atmos.
1319 Sci., 52(12), 2242–2257, 1995.
1320
1321 Wehner, B., Siebert, H., Stratmann, F., Tuch, T., Wiedensohler, A., Petäjä, T., Dal Maso, M. and
1322 Kulmala, M.: Horizontal homogeneity and vertical extent of new particle formation events, Tellus,
1323 Ser. B Chem. Phys. Meteorol., 59(3), 362–371, doi:10.1111/j.1600-0889.2007.00260.x, 2007.
1324
1325 Wonaschütz, A., Demattio, A., Wagner, R., Burkart, J., Zíková, N., Vodička, P., Ludwig, W.,
1326 Steiner, G., Schwarz, J. and Hitzenberger, R.: Seasonality of new particle formation in Vienna,
1327 Austria - Influence of air mass origin and aerosol chemical composition, Atmos. Environ., 118,
1328 118–126, doi:10.1016/j.atmosenv.2015.07.035, 2015.
1329
1330 Woo, K. S., Chen, D. R., Pui, D. Y. H. H. and McMurry, P. H.: Measurement of Atlanta aerosol
1331 size distributions: Observations of lutrafine particle events, Aerosol Sci. Technol., 34, 75–87,
1332 doi:10.1080/02786820120056, 2001.
1333
1334 Xiao, S., Wang, M. Y., Yao, L., Kulmala, M., Zhou, B., Yang, X., Chen, J. M., Wang, D. F., Fu, Q.
1335 Y., Worsnop, D. R. and Wang, L.: Strong atmospheric new particle formation in winter in urban
1336 Shanghai, China, Atmos. Chem. Phys., 15(4), 1769–1781, doi:10.5194/acp-15-1769-2015, 2015.
1337
1338 Yao, L., Garmash, O., Bianchi, F., Zheng, J., Yan, C., Kontkanen, J., Junninen, H., Mazon, S. B.,
1339 Ehn, M., Paasonen, P., Sipilä, M., Wang, M., Wang, X., Xiao, S., Chen, H., Lu, Y., Zhang, B.,
1340 Wang, D., Fu, Q., Geng, F., Li, L., Wang, H., Qiao, L., Yang, X., Chen, J., Kerminen, V. M.,
1341 Petäjä, T., Worsnop, D. R., Kulmala, M. and Wang, L.: Atmospheric new particle formation from
1342 sulfuric acid and amines in a Chinese megacity, Science, 361(6399), 278–281,
1343 doi:10.1126/science.aao4839, 2018.
1344
1345 Yli-Juuti, T., Nieminen, T., Hirsikko, A., Aalto, P. P., Asmi, E., Hörrak, U., Manninen, H. E.,
1346 Patokoski, J., Dal Maso, M., Petäjä, T., Rinne, J., Kulmala, M. and Riipinen, I.: Growth rates of
1347 nucleation mode particles in Hyytiälä during 2003-2009: Variation with particle size, season, data
1348 analysis method and ambient conditions, Atmos. Chem. Phys., 11(24), 12865–12886,
1349 doi:10.5194/acp-11-12865-2011, 2011.

1350 YPIEKA (Ministry for the Environment, Energy and Climate Change in Greece): Annual report of
1351 atmospheric pollution 2011, Ministry for the Environment, Energy and Climate Change in Greece,
1352 Department of Air Quality, April 2012,
1353 <http://www.ypeka.gr/LinkClick.aspx?fileticket=TYgrT0qoSrI%3D&tabid=490&language=el-GR>,
1354 last accessed 18/9/2019, 2012.
1355
1356 Ždímal, V., Smolík, J., Eleftheriadis, K., Wagner, Z., Housiadas, C., Mihalopoulos, N., Mikuška,
1357 P., Večeřa, Z., Kopanakis, I. and Lazaridis, M.: Dynamics of atmospheric aerosol number size
1358 distributions in the eastern Mediterranean during the “SUB-AERO” project, Water. Air. Soil
1359 Pollut., 214(1–4), 133–146, doi:10.1007/s11270-010-0410-4, 2011.
1360

1361 **TABLE LEGENDS:**

1362

1363 **Table 1:** Location and data availability (seasonal data availability is found in Table S4) of the
1364 sites in the present. In the studies referenced an extended description of the sites can be
1365 found.

1366

1367

1368 **FIGURE LEGENDS**

1369

1370 **Figure 1:** Map of the areas of study.

1371

1372 **Figure 2:** Frequency (a) and seasonal variation (b) of New Particle Formation events (Winter – DJF;
1373 Spring – MAM; Summer – JJA; Autumn – SON).

1374 **Figure 3:** Ratio of New Particle Formation event probability between weekends to weekdays. The
1375 greater the ratio the more probable it is for an event to take place during weekends
1376 compared to weekdays.

1377 **Figure 4:** Growth rate of particles up to 30 nm (with standard deviations) during New Particle
1378 Formation events at all sites.

1379 **Figure 5:** Seasonal variation of growth rate of particles up to 30 nm on New Particle Formation at
1380 (a) the rural background, (b) urban background and (c) roadside sites.

1381 **Figure 6:** Formation rate of 10 nm particles (J_{10}) (with standard deviations) from New Particle
1382 Formation at all sites.

1383 **Figure 7:** Seasonal variation of formation rate of 10 nm particles (J_{10}) (with standard deviations)
1384 from New Particle Formation events at (a) the rural background, (b) urban background
1385 and (c) roadside sites.

1386 **Figure 8:** (a) Number of region-wide New Particle Formation events per season and (b) fraction of
1387 region-wide events to total New Particle Formation events per season for each site.
1388 Region-wide events are considered those that occur on the same day on both background
1389 sites (Rural and Urban background).

1390 **Figure 9:** (a) NSF_{NUC} (average relative increase of ultrafine particles – particles of diameter up to
1391 100 nm) due to New Particle Formation events on event days) and (b) NSF_{GEN} (average
1392 annual relative increase of ultrafine particles due to New Particle Formation events) at all
1393 sites.

Table 1: Location and data availability (seasonal data availability is found in Table S4) of the sites in the present study. In the studies referenced an extended description of the sites can be found.

Site	Location	Available data	Meteorological data location	Data availability	Reference
DENRU	Lille Valby, 25 km W of Copenhagen, (55° 41' 41" N; 12° 7' 7" E) (2008 – 6/2010) Risø, 7 km north of Lille Valby, (55° 38' 40" N; 12° 5' 19" E) (7/2010 – 2017)	DMPS and CPC (5.8 - 700 nm, 65.4% availability), NO, NO _x , SO ₂ , O ₃ , minerals, OC, EC, NO ₃ ⁻ , SO ₄ ²⁻ , NH ₄ ⁺	Ørsted – Institute station	2008 – 2017	Ketzel et al., 2004
DENUB	Ørsted - Institute, 2 km NE of the city centre, Copenhagen, Denmark (55° 42' 1" N; 12° 33' 41" E)	DMPS and CPC (5.8 - 700 nm, 59.0% availability), NO, NO _x , O ₃ , minerals, EC	On site	2008 – 2017	Wang et al., 2010
DENRO	H.C. Andersens Boulevard, Copenhagen, Denmark (55° 40' 28" N; 12° 34' 16" E)	DMPS and CPC (5.8 - 700 nm, 65.0% availability), NO, NO _x , SO ₂ , O ₃ , minerals, OC, EC, NO ₃ ⁻ , SO ₄ ²⁻ , NH ₄ ⁺	Ørsted – Institute station	2008 – 2017	Wang et al., 2010
GERRU	Melpitz, 40 km NE of Leipzig, Germany (51° 31' 31.85" N; 12° 26' 40.30" E)	TDMPS with CPC (4.8 - 800 nm, 87.1% availability), OC, NO ₃ ⁻ , SO ₄ ²⁻ , NH ₄ ⁺ , Cl ⁻	On site	2008 – 2011	Birmili et al., 2016
GERUB	Tropos, 3 km NE from the city centre of Leipzig, Germany (51° 21' 9.1" N; 12° 26' 5.1" E)	TDMPS with CPC (3 - 800 nm, 88.0% availability)	On site	2008 – 2011	Birmili et al., 2016
GERRO	Eisenbahnstraße, Leipzig, Germany (51° 20' 43.80" N; 12° 24' 28.35" E)	TDMPS with CPC (4 - 800 nm, 64.4% availability)	Tropos station	2008 – 2011	Birmili et al., 2016
FINRU	Hyytiälä, 250 km N of Helsinki, Finland (61° 50' 50.70" N; 24° 17' 41.20" E)	TDMPS with CPC (3 – 1000 nm, 98.7% availability), NO, NO _x , SO ₂ , O ₃ , CO, CH ₄ , VOCs, H ₂ SO ₄	On site	2008 – 2011 & 2015 – 2018	Aalto et al., 2001
FINUB	Kumpula Campus 4 km N of the city centre, Helsinki, Finland (60° 12' 10.52" N; 24° 57' 40.20" E)	TDMPS with CPC (3.4 - 1000 nm, 94.0% availability)	On site	2008 – 2011 & 2015 – 2018	Järvi et al., 2009
FINRO	Mäkelänkatu street, Helsinki, Finland (60° 11' 47.57" N; 24° 57' 6.01" E)	DMPS (6 - 800 nm, 90.0% availability), NO, NO ₂ , NO _x , O ₃ , BC and SO ₂ from Kalio Station	Pasila station and on site	2015 – 2018	Hietikko et al., 2018
SPARU	Montseny, 50 km NNE from Barcelona, Spain (41° 46' 45" N; 2° 21' 29" E)	SMPS (9 – 856 nm, 47.7% availability), NO, NO ₂ , SO ₂ , O ₃ , CO, OM, SO ₄ ²⁻	On site	2012 - 2015	Dall'Osto et al., 2013
SPAUB	Palau Reial, Barcelona, Spain (41° 23' 14" N; 2° 6' 56" E)	SMPS (10.9 – 478 nm, 64.2% availability), NO, NO ₂ , SO ₂ , O ₃ , CO, BC, OM, SO ₄ ²⁻ , PM _{2.5} , PM ₁₀	On site	2012 – 2015	Dall'Osto et al., 2012

GRERU	Finokalia, 70 km E of Heraklion, Greece (35° 20' 16.8" N; 25° 40' 8.4" E)	SMPS (8.77 - 849 nm, 92.4% availability), NO, NO ₂ , O ₃ , OC, EC	On site	2012 – 2018	Kalkavouras et al., 2017
GREUB	“Demokritos”, 12 km NE from the city centre, Athens, Greece (37° 59' 41.96" N; 23° 48' 57.56" E)	SMPS (10 – 550 nm, 77.2% availability)	On site	2015 – 2018	Vassilakos et al., 2005

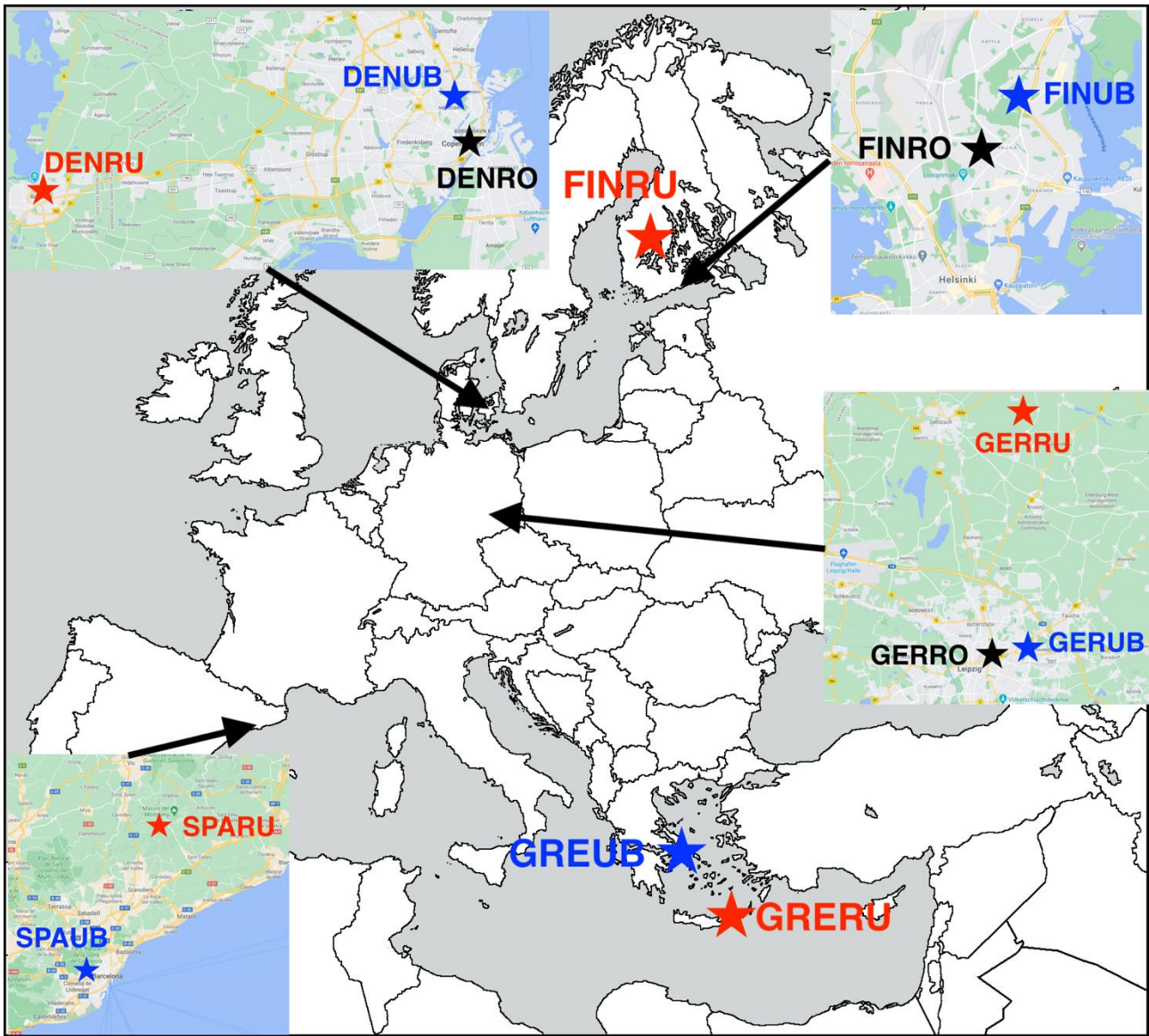
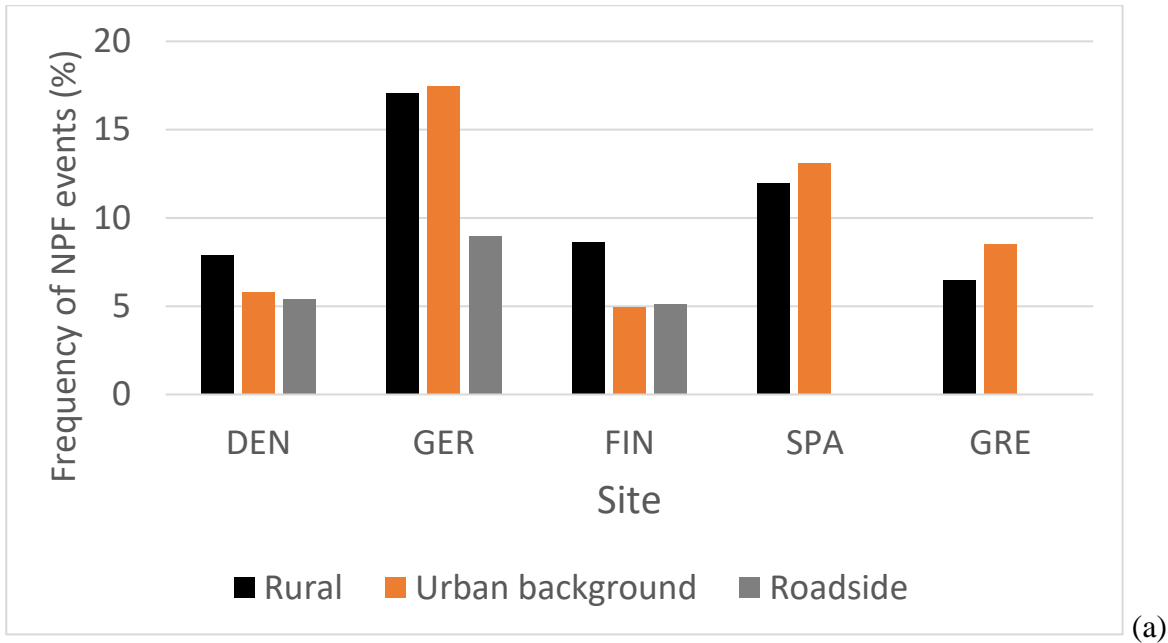


Figure 1: Map of the areas of study.



1405

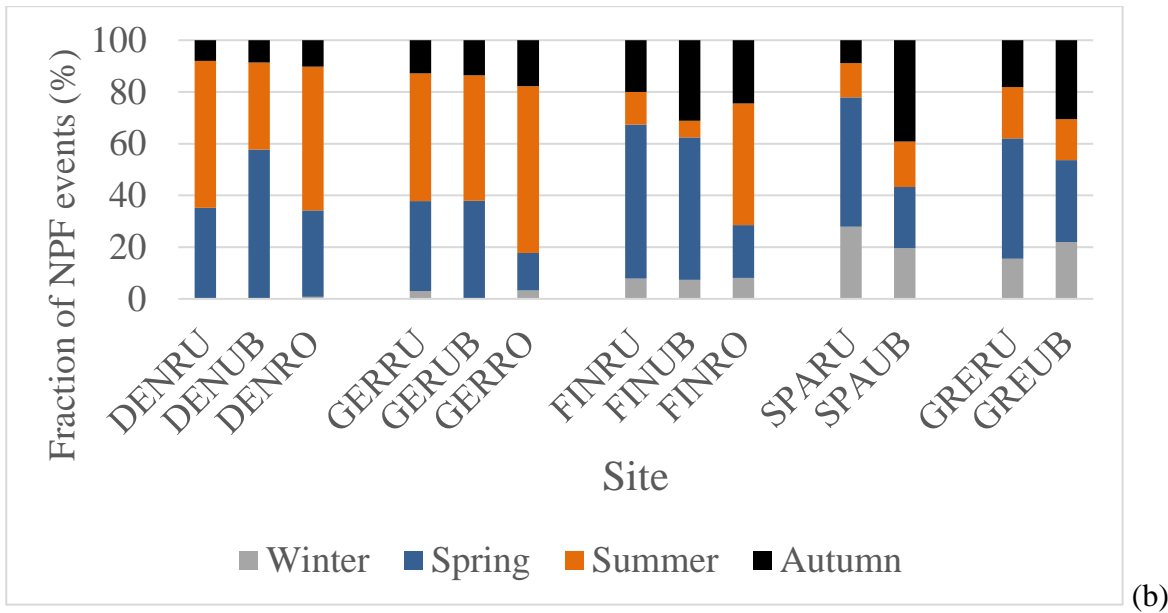


Figure 2: Frequency (a) and seasonal variation (b) of New Particle Formation events (Winter – DJF; Spring – MAM; Summer – JJA; Autumn – SON).

1410

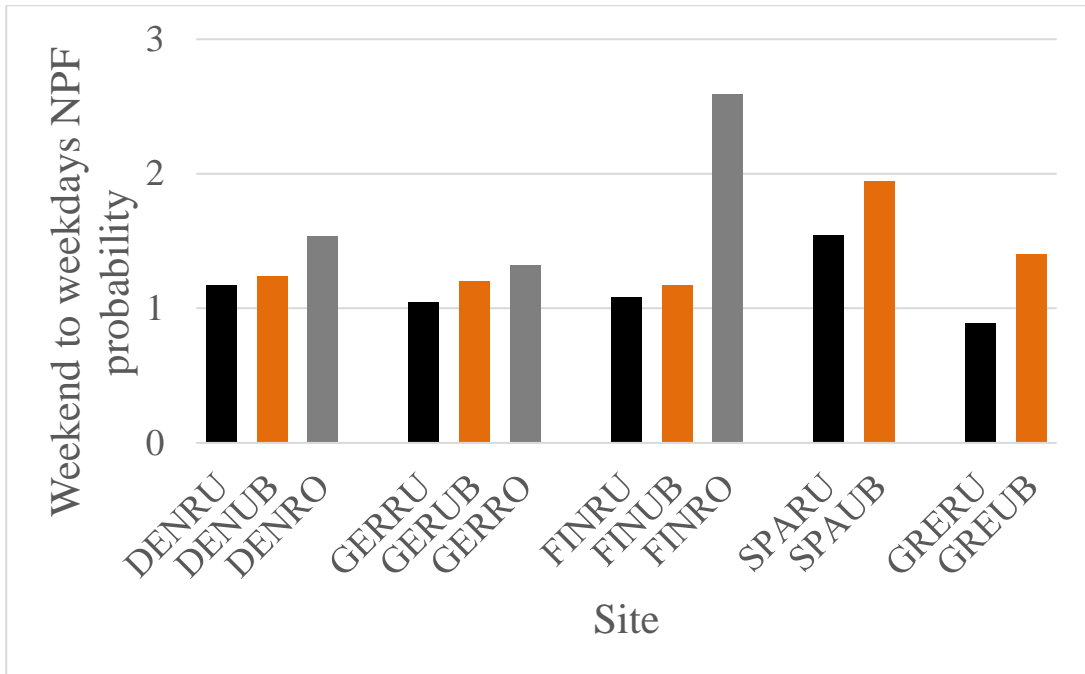
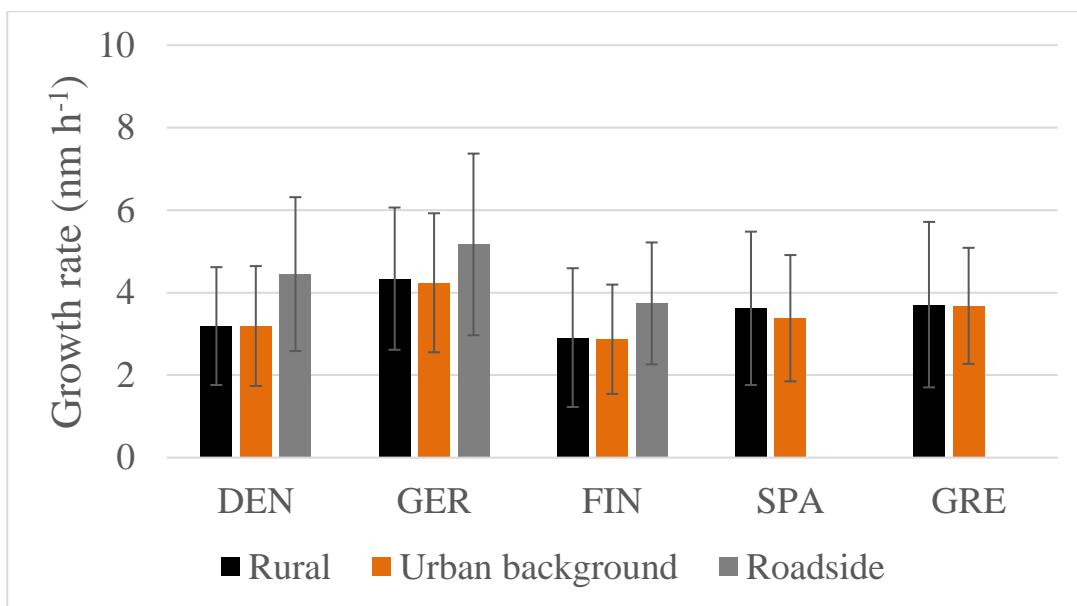
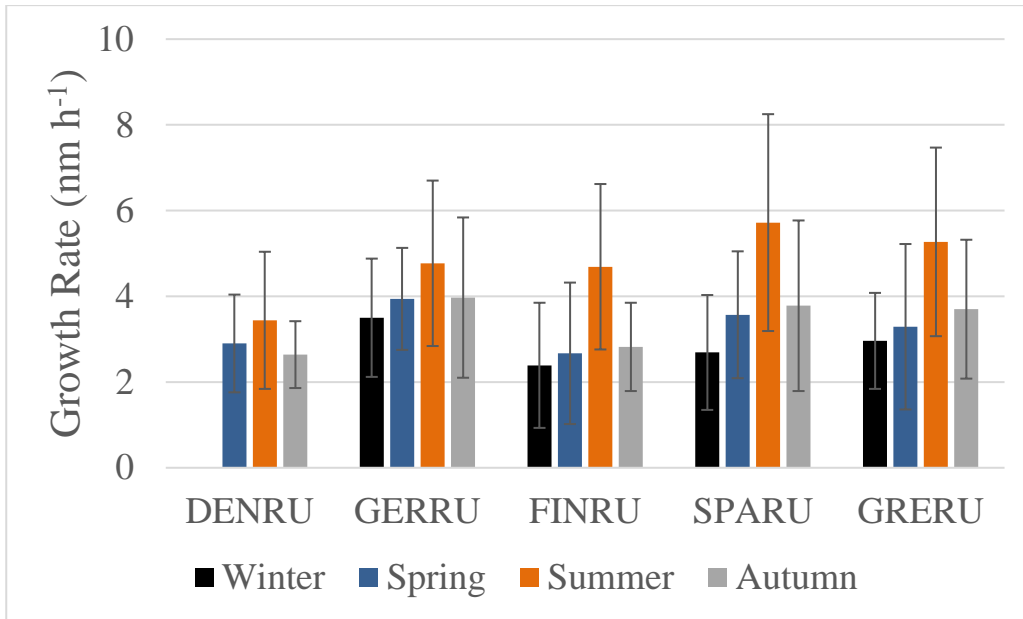


Figure 3: Ratio of New Particle Formation event probability between weekends to weekdays. The greater the ratio the more probable it is for an event to take place during weekends compared to weekdays.

1415

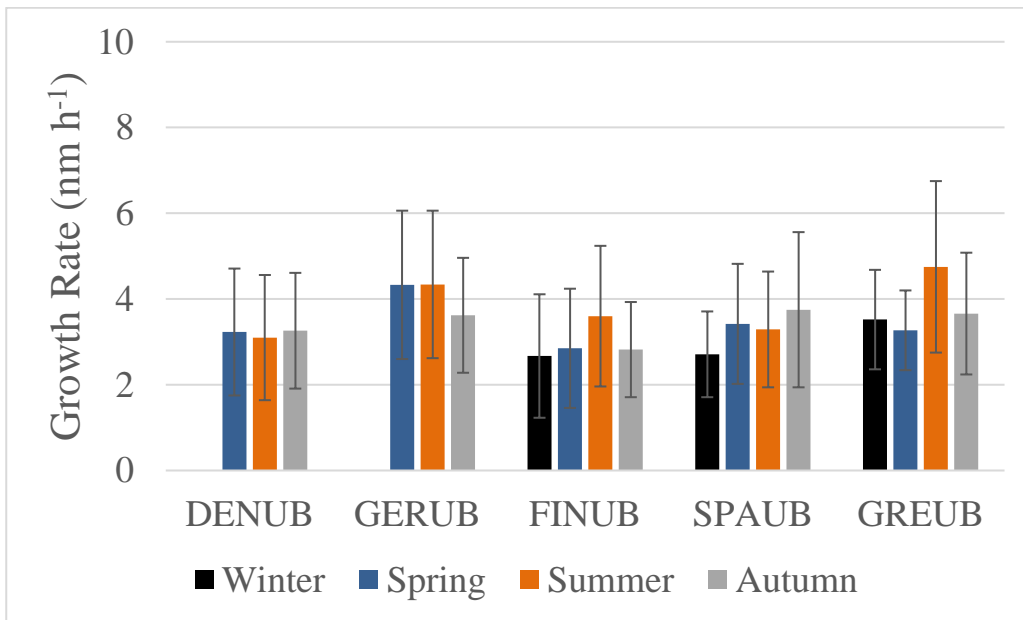


1420 **Figure 4:** Growth rate of particles up to 30 nm (with standard deviations) during New Particle Formation events at all sites.



(a)

1425



(b)

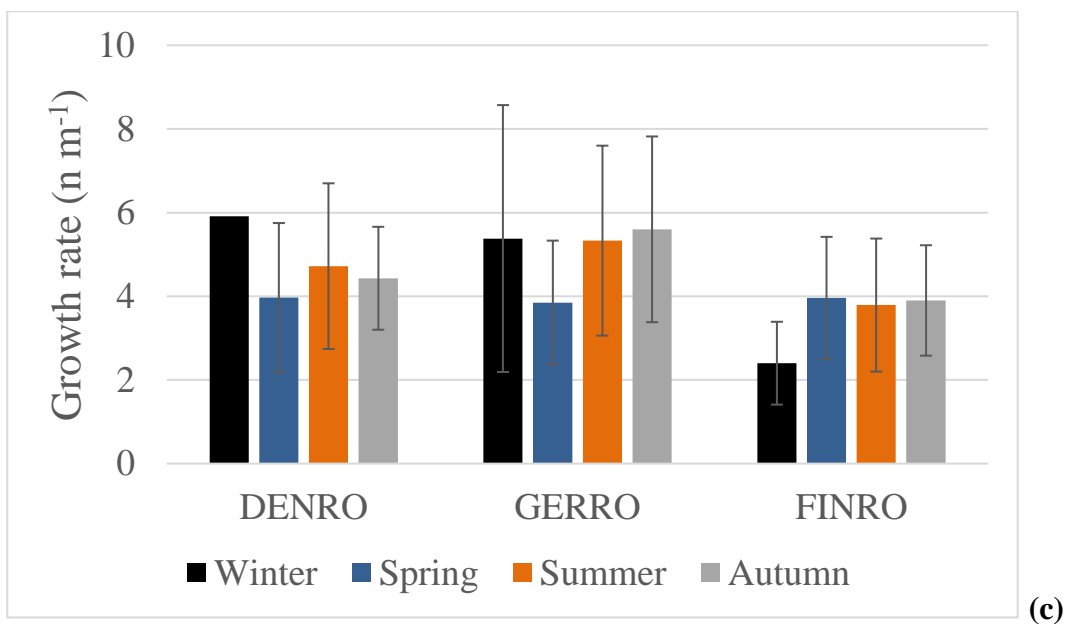
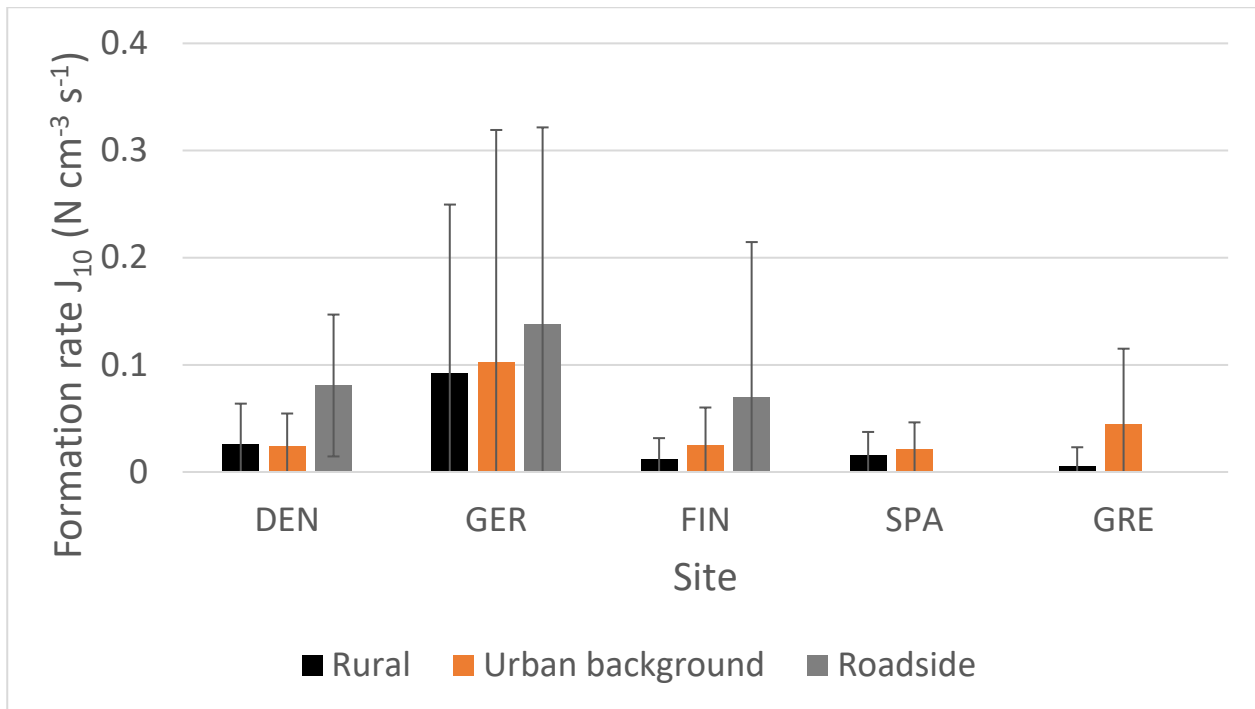
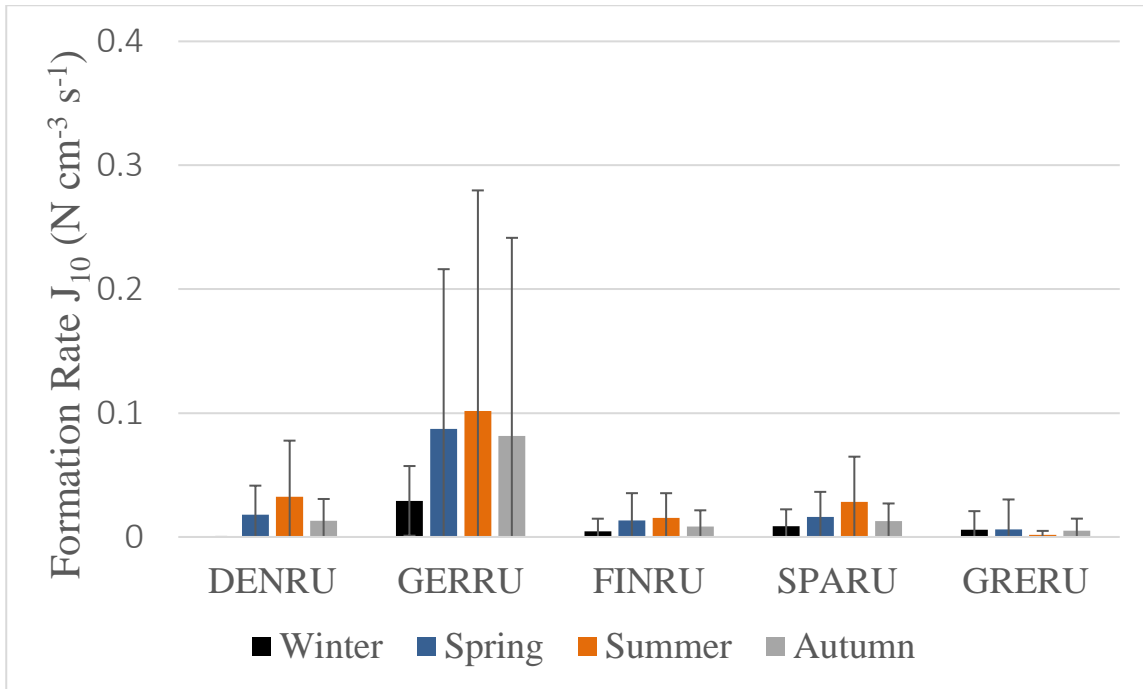


Figure 5: Seasonal variation of growth rate of particles up to 30 nm on New Particle Formation at 1430 (a) the rural background, (b) urban background and (c) roadside sites.



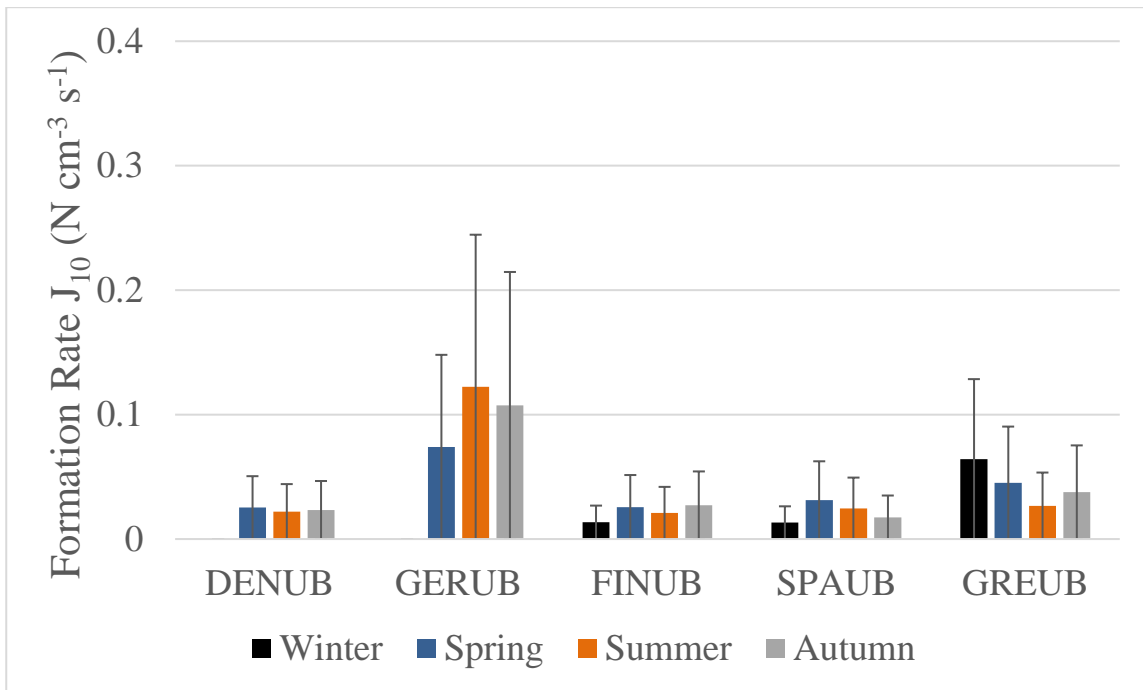
1435

Figure 6: Formation rate of 10 nm particles (J_{10}) (with standard deviations) during New Particle Formation events at all sites.



(a)

1440



(b)

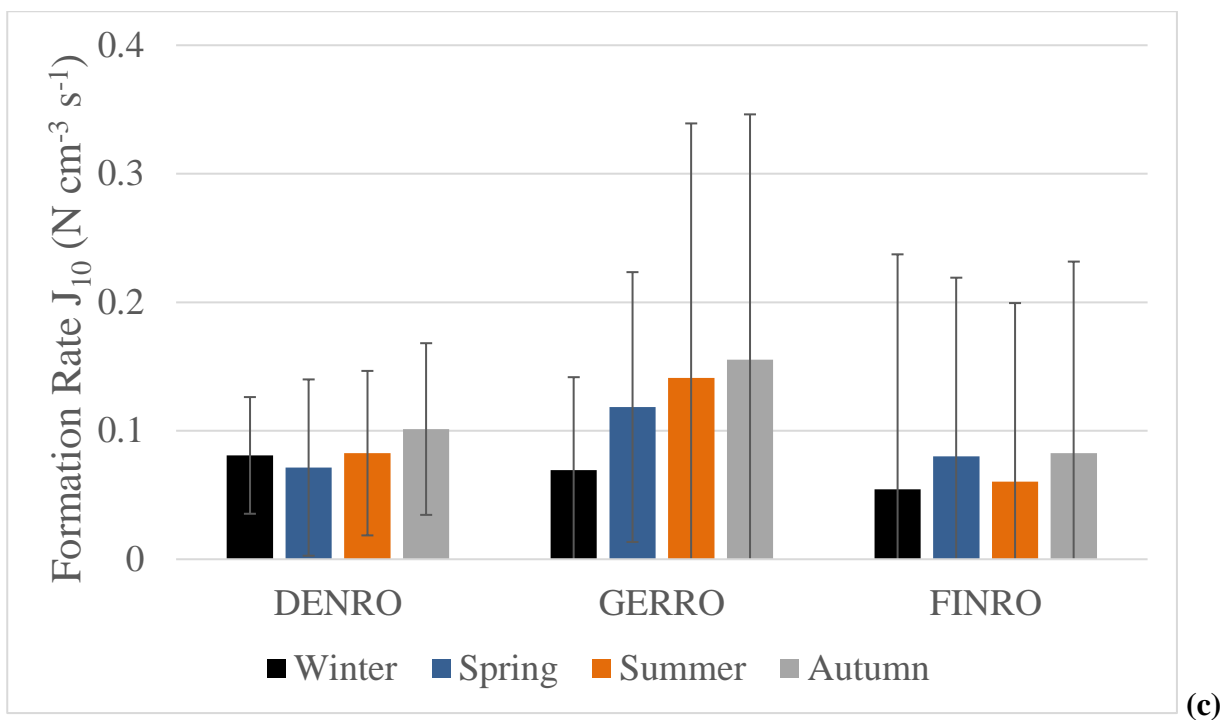
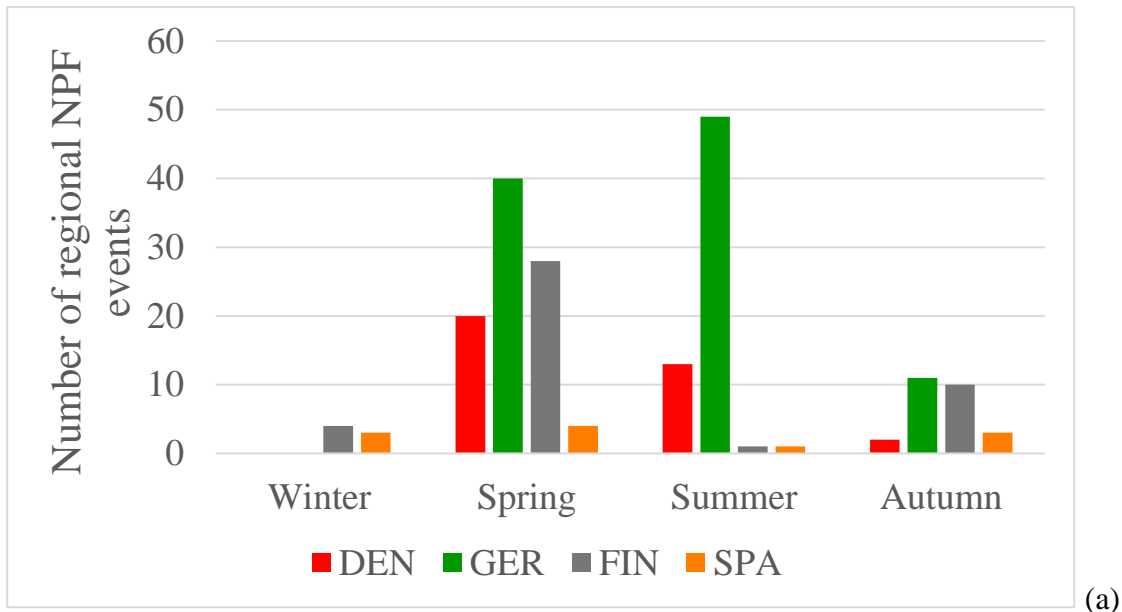
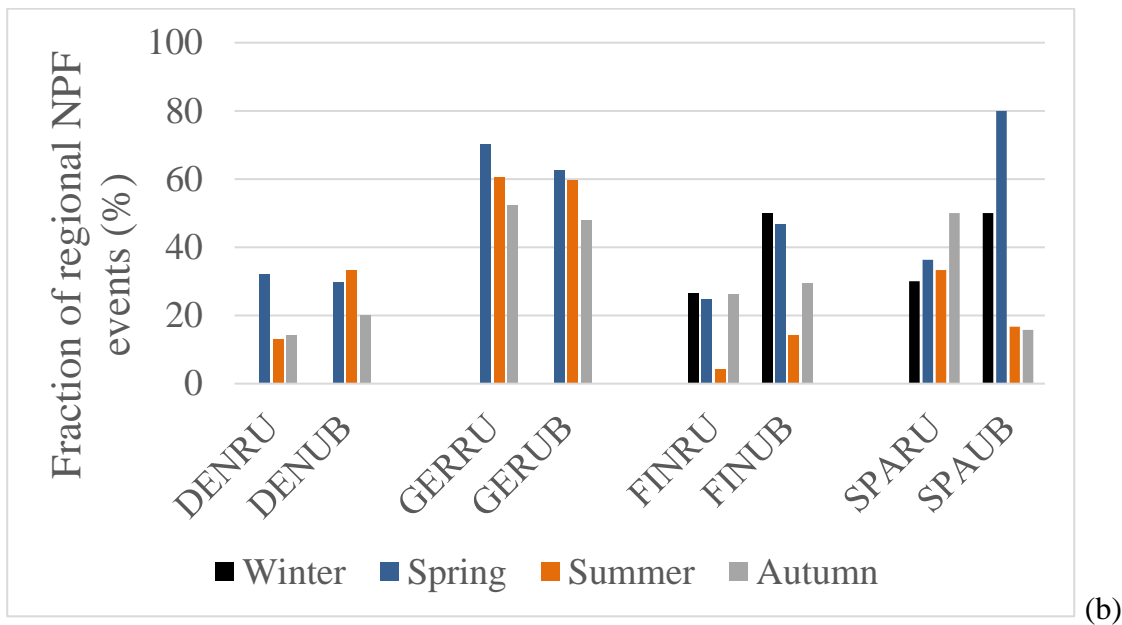


Figure 7: Seasonal variation of formation rate of 10 nm particles (J_{10}) (with standard deviations) from New Particle Formation events at (a) the rural background, (b) urban background and (c) roadside sites.

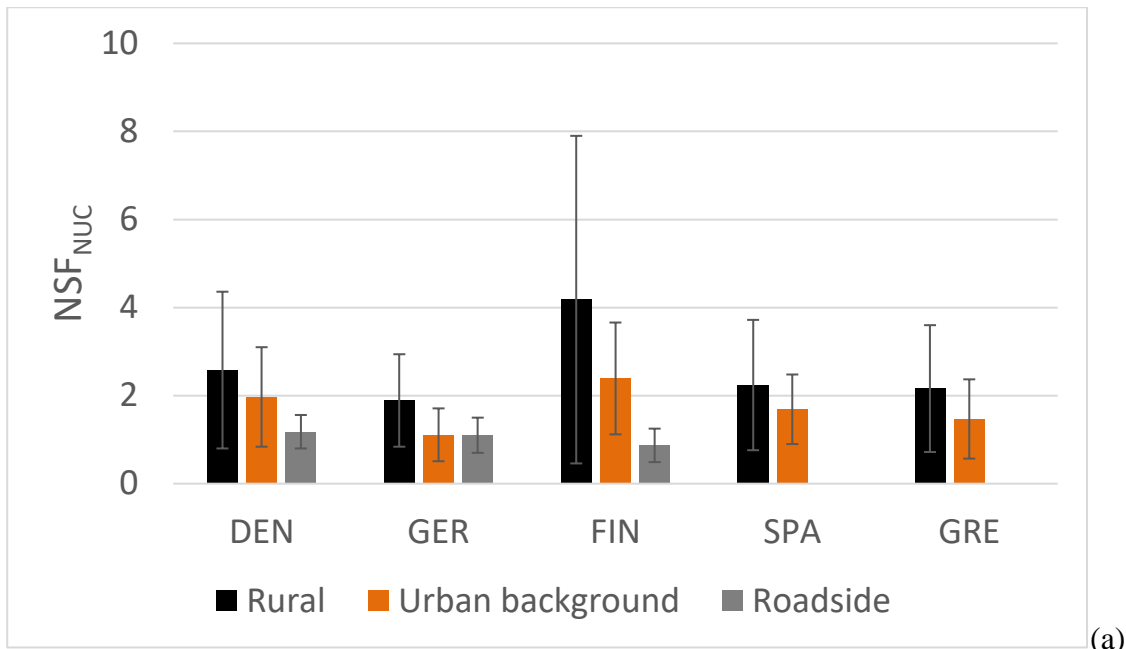


1450

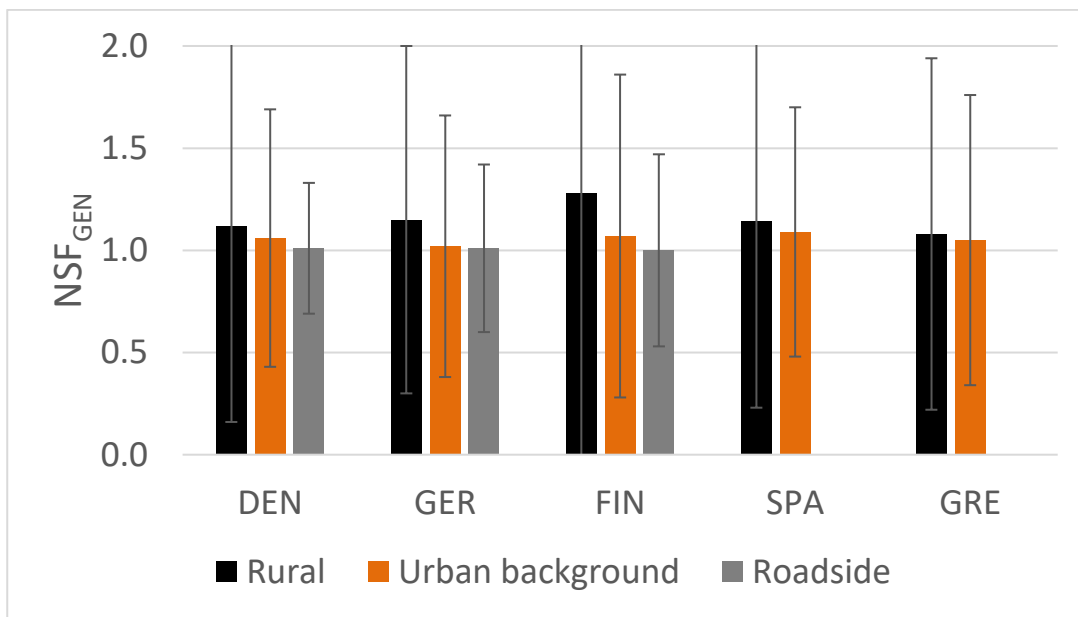


1455

Figure 8: (a) Number of region-wide New Particle Formation events per season and (b) fraction of region-wide events to total New Particle Formation events per season for each site. Region-wide events are defined as those that occur on the same day at both background sites (Rural and Urban background).



(a)



(b)

1460

Figure 9: (a) NSF_{NUC} (average relative increase of ultrafine particles – particles of diameter up to 100 nm) due to New Particle Formation events on event days) and (b) NSF_{GEN} (average annual relative increase of ultrafine particles due to New Particle Formation events) at all sites.